UNIVERSITY OF CALIFORNIA · ENGINEERING · LOS ANGELES

SEMI-ANNUAL TECHNICAL REPORT NO. 2

NEW TECHNIQUES FOR THE SYNTHESIS OF METALS AND ALLOYS

R. F. Bunshah

THE PROPERTIES OF RARE EARTH METALS AND ALLOYS

D. L. Douglass

D D C

OCT 26 1971

RECEIVED

F

10

DOCUMENT CONTROL DATA · R & D

(Security classification of title, body of abstract and indexing annotation must be entered when the overall report is classified)

1. ORIGINATING ACTIVITY *(Corporate author)*	2a. REPORT SECURITY CLASSIFICATION
School of Engineering & Applied Science University of California at Los Angeles Los Angeles, California 90024	Unclassified
	2b. GROUP

3. REPORT TITLE

I. NEW METHODS OF SYNTHESIS OF MATERIALS

II. THE PROPERTIES OF RARE EARTH METALS AND ALLOYS

4. DESCRIPTIVE NOTES *(Type of report and inclusive dates)*

Semi-Annual Technical Report, March 1, 1971 – July 31, 1971

5. AUTHOR(S) *(First name, middle initial, last name)*

I. R. F. Bunshah

II. D. L. Douglass

6. REPORT DATE	7a. TOTAL NO. OF PAGES	7b. NO. OF REFS
September 1, 1971	67	39

8a. CONTRACT OR GRANT NO.	9a. ORIGINATOR'S REPORT NUMBER(S)
AO #1643	
b. PROJECT NO.	UCLA ENG. 7161
c.	9b. OTHER REPORT NO(S) *(Any other numbers that may be assigned this report)*
d.	

10. DISTRIBUTION STATEMENT

Distribution of this document is unlimited

11. SUPPLEMENTARY NOTES	12. SPONSORING MILITARY ACTIVITY
	Advanced Research Projects Agency, Department of Defense

13. ABSTRACT

Two major areas of effort are encompassed:

I. <u>New Techniques for the Synthesis of Metals and Alloys.</u> The high rate physical vapor deposition (HRPVD) process is to be used for the following: 1) Preparation and characterization of Ni & Ni-20Cr alloy sheet. 2) Synthesis of compounds Y_2O_3, TiC, Si_3N_4 by reactive evaporation and their characterization. 3) Dispersion strengthened alloys, Ni-20Cr-Y_2O_3, Ni-20Cr-TiC and Ti-Y_2O_3. This report describes the synthesis of carbides, oxides and nitrides by reactive and activated reactive evaporation techniques.

II. <u>The Properties of Rare Earth Metals and Alloys.</u> The oxidation kinetics of Ni-20Cr containing nominally 1% of Y, Gd, or La have been evaluated over the range of 900 to 1200°C in static air. The nature of the oxide films formed and the disposition of the rare earth additions have been evaluated by X-ray diffraction and electromicroprobe analyses. Yttrium additions reduced the oxidation rate by a factor of about three, whereas Gd and La reduced the rate but by a lesser amount than yttrium. Oxide films formed at 1200°C consisted primarily of Cr_2O_3; spinels and NiO were observed at lower temperatures, 900 to 1000°C. The amount of the rare earths in the oxides was extremely small, although yttrium appeared to be concentrated at the oxide-gas interface on samples oxidized at 1200°C. No definite mechanism can be associated with the observations, although doping of the Cr_2O_3 films with a consommitant decrease in the cation vacancy concentration is consistent with the observations.

14. KEY WORDS	LINK A		LINK B		LINK C	
	ROLE	WT	ROLE	WT	ROLE	WT
Activated reactive evaporation						
Carbides						
Condensation						
Deposit						
Evaporation						
Evaporation apparatus						
Gadolinium						
High Rate Physical Vapor Deposition Process						
Lanthanum						
Lattice parameter						
Microhardness						
Nichrome						
Nickel						
Nitrides						
Oxidation						
Oxides						
Oxidation mechanism						
Rare-earch additions						
Reactive evaporation						
Refractory carbides						
Scale formation						
Silicon nitride-Si_3N_4						
Substrate						
Synthesis of Materials						
Thickness distribution						
Titanium carbide						
Yttria-Y_2O_3						
Yttrium						

SEMI-ANNUAL TECHNICAL REPORT NO. 2

I.   New Techniques for the Synthesis of Metals and Alloys
     (Principal Investigator - Professor R. F. Bunshah)

     Office Phone: (213) 825-2210 or 825-5473

II. The Properties of Rare Earth Metals and Alloys
     (Principal Investigator - Professor D. L. Douglass)

     Office Phone: (213) 825-1622 or 825-5534

Materials Department
School of Engineering and Applied Science
University of California
Los Angeles, California

TABLE OF CONTENTS

INTRODUCTION

PART I

New Techniques for the Synthesis of Metals and Alloys
(Tasks I, II, III)

PART II

Properties of Rare-Earth Metals and Alloys
(Task IV)

ABSTRACT

Two major areas of effort are encompassed:

I. New Techniques for the Synthesis of Metals and Alloys

The high rate physical vapor deposition (HRPVD) process is to be used for the following:

1. Preparation and characterization of Ni and Ni-20Cr alloy sheet,

2. Synthesis of compounds Y_2O_3, TiC, Si_3N_4 by reactive evaporation and their characterization.

3. Dispersion strengthened alloys, Ni-20Cr-Y_2O_3, Ni-20Cr-TiC and Ti-Y_2O_3.

This report describes the synthesis of carbides, oxides and nitrides by reactive and activated reactive evaporation techniques.

II. The Properties of Rare Earth Metals and Alloys

The oxidation kinetics of Ni-20Cr containing nominally 1% of Y, Gd, or La have been evaluated over the range of 900 to 1200°C in static air. The nature of the oxide films formed and the disposition of the rare earth additions have been evaluated by X-ray diffraction and electronmicroprobe analyses.

Yttrium additions reduced the oxidation rate by a factor of about three, whereas, Gd and La reduced the rate but by a lesser amount than yttrium. Oxide films formed at 1200°C consisted primarily of Cr_2O_3; spinels and NiO were observed at lower temperatures, 900 to 1000°C. The amount of the rare earths in the oxides was extremely small, although yttrium appeared to be concentrated at the oxide-gas interface on samples oxidized at 1200°C. No definite mechanisms can

be associated with the observations, although doping of the Cr_2O_3 films with a concommitant decrease in the cation vacancy concentration is consistent with the observations.

INTRODUCTION

This report describes research activities on ARPA Grant No. AO 1643. The scope of the work is divided into two major areas of effort and further subdivided into four tasks as shown below.

1. New Techniques for the Synthesis of Metals and Alloys - Tasks I, II, and III. (Professor R. F. Bunshah - Principal Investigator)

2. The Properties of Rare Earth Metals and Alloys - Task IV. (Professor D. L. Douglass - Principal Investigator)

In the following each of the two topics will be described separately as Part I and Part II of this report with the progress to date.

PART I

NEW TECHNIQUES FOR THE SYNTHESIS OF METALS AND ALLOYS
(TASKS I, II, AND III)

R. F. Bunshah

I. Background

High rate physical vapor deposition (HRPVD) techniques[1-8] are to be used to prepare metallic alloys, ceramics, and metal-ceramic mixtures (dispersion strengthened alloys). The method consists of evaporation of metals, alloys and ceramics contained in water cooled crucibles using high power electron beams. The process is carried out in a high vacuum environment. The use of high power electron beams makes it possible to produce very high evaporation rates. The vapors are collected on heated metallic substrates to produce full density deposits at high deposition rates.

There are three tasks in this section:

Task I: The preparation and characterization of Nickel and Ni-20Cr alloy sheet by the high rate physical vapor deposition process.

Task II: Synthesis and characterization of compounds by Reactive Evaporation. The compounds to be prepared are Y_2O_3, TiC and Si_3N_4.

Task III: Dispersion strengthened alloys produced by HRPVD Process, and their characterization. The specific alloys to be studied are:

A. $Ni-20Cr-Y_2O_3$ B. $Ni-20Cr-TiC$ C. $Ti-Y_2O_3$

Single source and two source evaporation methods will be used to produce these alloys.

The HRPVD process has several attractive features:

A. Simple, full density shapes (sheet, foil, tubing) can be produced at high deposition rates, 0.001" per minute thickness increment thus making it an economically viable process.

B. Metals and alloys of high purity can be produced.

C. Very fine grain sizes (1μ grain diameter or smaller) can be produced by controlling substrate temperature. Grain size refinement is

produced by lowering the condensation temperature.

D. An alloy deposit may be produced from a single rod fed source.
This occurs because the molten pool at the top of the rod is about
1/4" deep only. The vapor composition is the same as that of the
solid rod being fed into the molten pool. At equilibrium, the
composition of the molten pool differs from that of the vapor or the
solid feed. It is richer in those components having a low vapor
pressure. The composition of the vapor is the product of the vapor
pressure times the mole fraction of the component. For example, a
Ti-6Al-4V alloy deposit where the differences in vapor pressure of
Al and V are a factor of 5,000 at 1600°C can be produced by evapora-
tion from a single source. The feed-rod is Ti-6Al-4V and the molten
pool is much richer in V than in Al.

E. Two or more sources can be used to simultaneously deposit on
the same substrate thus conferring the ability to produce complex
alloys. For example, an alloy with a 2 or 3 component solid solution
matrix may be evaporated from one source and another metal or ceramic
for the dispersed phase from another source. The dispersion size
and spacing should be very fine since the deposition is occurring from
the vapor phase.

The unique feature of this process is that all of the above benefits
can be obtained simultaneously.

It should be noted that the condensation temperature is a very
important process variable. Bunshah and Juntz[8] found that for
titanium, as the deposition temperature is lowered the grain size of
the fully dense deposit becomes finer. At very low temperatures
($\sim$ 25% of the melting point) the deposit has less than full density.

Since a fine grain sized microstructure represents an optimum condition
of strength and toughness in a material, the importance of control over
the   deposition temperature becomes obvious.

II. Scope of work and progress in reporting period (February 1-July 31, 1971)

The main tasks on this contract are the preparation and testing
of the various alloys, ceramics and dispersion strengthened alloys as
outlined in Section I above. Very essential to the preparation of
suitable test specimens are two other factors:

A. Design of the apparatus for high rate physical vapor deposition.

B. Theoretical calculation of the thickness distribution and temperature
distribution of the deposited material which is in this case in the
form of a sheet.

Both of these tasks are essential preliminaries to the main
scope of work. They were completed and described in semi-annual
technical report No. 1.[9]

Two papers based on item B above have been submitted and
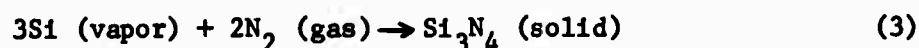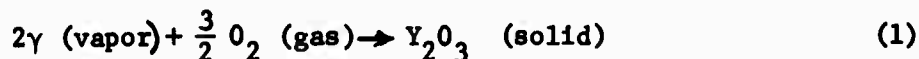accepted for publication.[10,11]

In this reporting period the following work was carried out.

A. Installation of the high rate physical vapor deposition apparatus
was concluded. On testing, it had some leaks due to bad welds and
some parts had to be returned to the manufacturer for repairs. It will
be reinstalled and tested in the next reporting period.

B. Theoretical model for alloy evaporation from a single rod-fed
electron beam source. This model relates the various aspects of the
problem concerned with the deposition of an alloy of desired composition

from a feed-rod of the same composition. The model will be experi-
mentally tested in the next six months and reported on in the progress
report due then.

C. Feasibility studies on the synthesis of Y_2O_3, TiC and Si_3N_4 by
reactive evaporation.

The major emphasis on experimental effort during this period was
devoted to a feasibility study of the synthesis of compounds by reactive
evaporation at high deposition rates (2μm/min and higher). The
experiment consists of evaporating the metal from an electron beam
heated source at high rates in the presence of an appropriate partial
pressure of a reactive gas. The desired reactions are:

$$2\gamma \text{ (vapor)} + \frac{3}{2} O_2 \text{ (gas)} \rightarrow Y_2O_3 \text{ (solid)} \qquad (1)$$

$$2Ti \text{(vapor)} + C_2H_2 \text{ (gas)} \rightarrow 2TiC \text{ (solid)} + H_2 \text{ (gas)} \qquad (2)$$

$$3Si \text{ (vapor)} + 2N_2 \text{ (gas)} \rightarrow Si_3N_4 \text{ (solid)} \qquad (3)$$

Preliminary experiments with the synthesis of Y_2O_3 and TiN (instead
of Si_3N_4) showed that synthesis of these compounds at high rates by
reactive evaporation was possible. In the case of TiC, no synthesis
by reactive evaporation was achieved. Therefore, a new process of
Activated Reactive Evaporation previously conceived[12] was applied
and the synthesis of TiC at high rates was successfully achieved.
The studies on this task have been very successful and the subject is
treated in detail in Supplement 1 to this part of the report.

III. Future Work

In the next half-year period, the following work is scoped.
A. Reinstallation and commissioning of the two source high vacuum high
rate physical vapor deposition apparatus.

B. Experimental verification of the model for alloy evaporation
from a single source using the Ni-20Cr alloy.

C. Continuation of the work on synthesis and testing of compounds
Y_2O_3, TiC and Si_3N_4 by reactive and activated reactive evaporation.

D. Deposition of Ni and Ni-20Cr alloy sheets and study of their
structure and properties.

E. Feasibility studies on production of Ni-20Cr alloys containing
dispersed phases by HRPVD processes from two evaporation sources.

IV. Personnel

The following personnel have been working on this project
in this reporting period.

Principal Investigator - Professor R. F. Bunshah

Graduate Students - Mr. Raymond Chow (up to April 30, 1971) and
  Mr. Rao Nimmagadda.

Post Doctoral Fellow - Dr. A. C. Raghuram (from February 1, 1971)

Undergraduate Student - Mr. Neil Kane (from June 1, 1971)

Technician - Mr. Fred Weiler

REFERENCES

1. Bunshah, R. F., "Superpurification of Metals by Vacuum Distillation: A Theoretical Study," Trans. Vac. Met. Conf., 1963, AVS, 121.

2. Bunshah, R. F., and Juntz, R. S., "Purification of Beryllium by Crucible Free Melting and Distillation Process" in Beryllium Technology, Gordon and Breach, 1964, 1.

3. Bunshah, R. F., "Impurity Removal by Distillation of Beryllium from the Solid State," Proceedings, Int'l. Conf. on Beryllium, Grenoble, France, 1965, Presses Universitaries de France, 108 Blvd. St. Germain, Paris, 6, 63.

4. Bunshah, R. F., and Juntz, R. S., "The Purification of Beryllium by Vacuum Melting followed by Vacuum Distillation in an Electron Beam Furnace with Simultaneous deposition of Sheet," Trans. Vac. Met. Conf., 1966, AVS, 209.

5. Bunshah, R. F., "The Effect of Purification on Some Mechanical Properties of Beryllium," Metals Engineering Quarterly, Nov. 1964, 8.

6. Bunshah, R. F., and Juntz, R. S., "Electron Beam Distillation Furnace for Reactive Metals: Design Considerations and Operating Experience," Trans. Vac. Met. Conf., 1965, AVS, 200.

7. Bunshah, R. F. and Juntz, R. S., "Design Considerations for the Production of Massive Deposits of Alloys by Evaporation from Multiple Electron Beam Heated Sources," Trans. Vac. Met. Conf., 1967, AVS, 799.

8. Bunshah, R. F., and Juntz, R. S., "Influence of Condensation Temperature on Microstructure and Mechanical Properties of Titanium Sheet," to be published.

9. Bunshah, R.F., and Douglass, D. L., Technical Report - UCLA-Eng-7112, March, 1971.

10. Nimmagadda, R., and Bunshah, R. F., to be published in J. Vac. Sc. and Tech., December 1971.

11. Chow, R., and Bunshah, R. F., to be published in J. Vac. Sci. and Tech., Dec., 1971.

12. Bunshah, R. F., Patent Disclosure, November 1970.
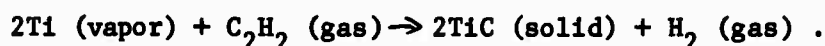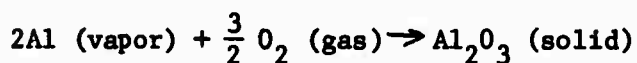
Supplement - 1

High Rate Physical Vapor Deposition of Compounds by Reactive Evaporation
and Activated Reactive Evaporation

I. Introduction

Many compounds have very desirable properties either when used by them-
selves as monolithic structures or when incorporated with other materials, e.g.,
dispersed phases in high temperature high strength alloys, as hard coatings
on tough substrates as in tooling, etc.

If it is desired to deposit compounds from the vapor phase onto a
stustrate, one has a choice of several processes:

1. Sputtering of the compound from a target of the same composition.

2. Direct evaporation of the compound from an evaporation source of the
same composition.

3. Reactive evaporation in which metal vapor atoms from an evaporation source
containing the appropriate metal react with the reactive gas atoms present
in the vapor phase to form compounds; e.g.

$2Al$ (vapor) $+ \frac{3}{2} O_2$ (gas) $\rightarrow Al_2O_3$ (solid)

$2Ti$ (vapor) $+ C_2H_2$ (gas) $\rightarrow 2TiC$ (solid) $+ H_2$ (gas) .

There are two considerations which govern the choice of the process:

1. The ability to deposit compounds of the desired composition and
structure.

2. The rate of deposition which may affect the economics of the process.

Most compounds can be deposited by sputtering. However, it has two
possible disadvantages.

1. Break-up of the compound into fractions which may or may not recombine
to yield the desired composition in the deposit. This is not too often
the case.

2. A low deposition rate, usually of the order of 0.1µm/min which can be accelerated to 1µm/min but with the attendent problem of incorporation of the sputtering gas into the deposit.

Direct evaporation of compounds is possible but also suffers from two possible disadvantages.

1. Compounds of technical interest usually have a very high melting point (> 2,500°C) which necessitates the use of a high density heat source to produce appreciable evaporation rates.

2. The possible break-up of the compound into fractions during evaporation.

On the other hand, with reactive evaporation, the evaporant is a metal whose melting point is lower than the metal compound and therefore higher metal atom densities in the vapor phase are easier to produce. Thus, high deposition rates, i.e., rates greater than 0.1 mil = 2.5µm = 25,000 Å per minute are possible.

Two possible problems with reactive evaporation are:

1. The kinetics of the reaction in the vapor phase to form the compound.

2. Control of the chemical composition of the compound. This could be a problem or alternately could add to the versatility of the process, since one could vary the stoichiometry (e.g., carbon/metal ratio in carbides) of the compound and hence vary the properties.

In this investigation, we will emphasize the reactive evaporation and also carry out direct evaporation of compounds for comparative purposes.

II. High rate physical vapor deposition of compounds by reactive evaporation, and activated reactive evaporation

In reactive evaporation metal vapor atoms react with gas atoms present in the atmosphere to form compounds. For example, aluminum metal atoms in the vapor phase combine with oxygen in the gas phase to form aluminum oxide.

$$2 \text{ Al (vapor)} + \frac{3}{2} O_2 \text{ (gas)} \rightarrow Al_2O_3 \text{ (solid)}$$
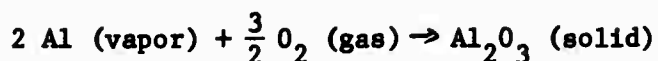
Similarly, titanium reacts with a hydrocarbon gas, e.g., acetylene to form titanium carbide, e.g.,

$$2Ti \text{ (vapor)} + C_2H_2 \text{ (gas)} \rightarrow 2TiC \text{ (solid)} + H_2 \text{ (gas)}$$
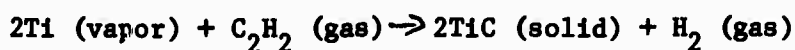
Examples of reactive evaporation in the literature are as follows:

1. Brinsmaid, Keenan, Koch and Parsons[1] deposited thin films of TiO_2 by evaporation of titanium from a resistance heated source in the presence of pure O_2 at a pressure of 2.10^{-4} to 1.10^{-3} torr.

2. Auwarter[2] produced thin films of various oxides by evaporation of the metal or oxide from resistance heated sources in the presence of a partial pressure of oxygen. The oxide films produced are, SiO_2, TiO_2, Al_2O_3, ZnO, SnO_2, ZrO_2 and Fe_2O_3.

3. Herrick and Tevebaugh[3] deposited copper oxide films by vaporization of copper from resistance heated sources in an oxygen atmosphere.

4. Novice et al[4] and Schilling[5] deposited Al_2O_3 films by reactive evaporation from resistance heated aluminum source in the presence of oxygen.

5. Ritter[6] produced thin films of Si_2O_3 and TiO_2 by reactive evaporation of Si, Ti, SiO and TiO from resistance heated sources in the presence of 10^{-4} to 10^{-3} torr oxygen.

6. Rairden[7] prepared thin films of NbN and TaN by evaporation of Nb and Ta from an electron beam heated source in an N_2 partial pressure of 10^{-4} to 10^{-3} torr, and AlN by evaporation of Al in NH_3 atmosphere.[8]

7. Ferrien and Pruniaux[9] produced Al_2O_3 by reactive evaporation of Al in an atmosphere of water vapor at 10^{-1} torr in the reaction zone.

8. Learn and Haq[10] produced β SiC by reactive evaporation of Si in C_2H_2 atmosphere.

In all these cases, only thin films were produced at very low deposition rates ($\leqslant 0.2\mu m/min$).
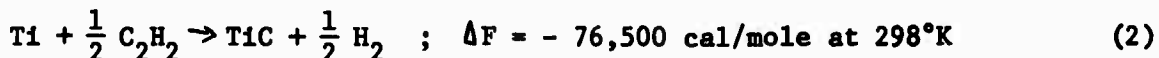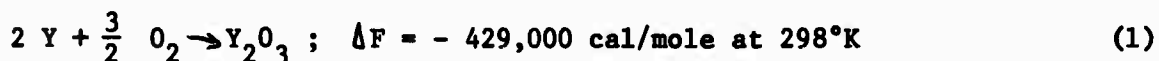
4. High reaction probability can be obtained in many instances only by activating the reactants i.e., the metal and gas atoms.

Activation of the reaction can occur naturally or be artificially stimulated. Several natural factors undoubtedly influence the process. For example,

1. High free energy of formation of the compound would tend to activate the process and contribute to high reaction efficiency.

2. The more complex the gas species involved in the reaction, the smaller the probability of a high reaction efficiency; e.g., if the reacting gas is a simple molecule like O_2 the reaction efficiency might be expected to be higher than if a more complex molecule like C_2H_2 were involved.

3. Removal of the reaction products from the reaction interface.

Consider the two reactions for the compound formation,

$$2 \ Y + \frac{3}{2} \ O_2 \rightarrow Y_2O_3 \ ; \quad \Delta F = -429,000 \text{ cal/mole at } 298°K \qquad (1)$$

$$Ti + \frac{1}{2} \ C_2H_2 \rightarrow TiC + \frac{1}{2} \ H_2 \ ; \quad \Delta F = -76,500 \text{ cal/mole at } 298°K \qquad (2)$$

The free energy of formation, ΔF, is more favorable for reaction (1) than for reaction (2). Reaction (2) also has a more complex reactive gas species than reaction (1), i.e., C_2H_2 vs. O_2. Reaction (2) can also be driven in the reverse direction by increase of H_2 partial pressure in the reaction zone, which is why the removal of reaction products from the reaction interface is important. This does not apply to reaction (1).

For all these reasons, one might expect the kinetics or reaction efficiency for the formation of Y_2O_3 by reactive evaporation to be more favorable than those for TiC.

In our experiments, the synthesis and high rate deposition of Y_2O_3 by reactive evaporation was readily achieved whereas evaporation of Ti

Reactive evaporation processes can be limited by the kinetics of the reaction taking place. The efficiency or yield of the reaction can be very low thus resulting in very low deposition rates, $\sim$ 0.1 micron per minute or less at source to substrate distance of 8 to 10 inches typically.

For high deposition rates, one must have several necessary conditions:

1. Adequate supply of metal vapor atoms.

2. Adequate supply of gas atoms.

3. A high efficiency or yield of the reaction.

The third item mentioned above necessitates two steps:

1. High rate of collision between metal and gas atoms in the vapor phase, i.e., a sufficiently high vapor pressure of both species. The collisions can also occur on the substrate.

2. High reaction probability (close to 100%) when such collisions occur.

All of these conditions need to be simultaneously met in the experiment to successfully deposit compounds at high depositions rates. For example,

1. An adequate supply of metal atoms in the vapor phase can be obtained by using a high rate evaporation source such as an electron beam heated source. The electron beam provides a high density heat source focused onto the surface of the metal in the liquid pool. This does not exclude other high rate evaporation sources such as induction heated or laser heated sources.

2. An adequate supply of gas atoms is provided by having a sufficiently high partial pressure of gas atoms in the gas phase, e.g., partial pressure of 10^{-4} torr or higher.

3. A high collision rate between metal and gas atoms in the vapor phase or on the substrate. This is assumed by the high partial pressures of metal and gas atoms.

in the presence of a reactive gas such as C_2H_2 failed to produce TiC. The experimental details are discussed in section IV.

For the synthesis of TiC, the Actived Reactive Evaporation Process using electron beam evaporation of the metal species (in this case titanium) was developed.[11] Reactions can be activated by energizing the reactants, or in terms used in chemical kinetics, converting the reactants to their activated states. Activation of the reactants can be carried out either before the reactants are brought together or directly in the reaction zone. The latter alternative would be expected to yield much higher reaction efficiencies since in the former case there is ample opportunity for the activated reactants to become deactivated prior to reaction by collision with surfaces, e.g., the walls of the tubes rised to convey gases, etc.

A glow discharge or a microwave discharge can be used to activate vapor phase species and thus accelerate the reaction. There are a number of examples in the literature where activation of the gaseous species was carried out outside the reaction zone. They are as follows:

1. Auwarter[2] studied the deposition of thin film oxides of Si, Zr, Ti, Al, Zn, Sn by reactive evaporation of the metal from resistance heated sources in a partial pressure of oxygen gas. Ionization of the oxygen gas outside the reaction zone by glow discharge between two electrodes is claimed to increase the "affinity" between the gas ion and the metal compound, i.e., enhance the probability of formation of metal compounds. Deposition rates of about $0.2\mu m$ per minute were obtained.

2. Wank and Winslow[12] deposited films of AlN by evaporating Al from a r.f. heated BN crucible and reacting the Al deposited on the substrate with N_2 gas which has been dissociated by a $60H_z$ a.c. discharge at the end of the gas feed tube. Deposition rates of 0.1 to $0.2\mu m$ per min were obtained.

3. Kosicki and Kahing[13] produced GaN thin-films by depositing pure Ga from a resistance heated source onto a substrate in the presence of activated N_2 gas. The N_2 gas was made chemically active by partial dissociation in a microwave discharge located away from the source and the substrate. Deposition rates of 0.2 to 0.3μm per minute were obtained.

From the above examples, for the high rate synthesis and deposition of compounds (⩾ 2.5μm per minute), it is reasonable to conclude that activation of all the reactants in the reaction zone is essential. Several experimental arrangements can be conceived using an appropriate heat source such as electron beam or laser heating to produce the high metal vapor flux, a high flux of reactive gas molecules, and a glow discharge or microwave discharge in the reaction zone. The one used in this investigation is described in the next section.

III. Activated reactive evaporation using an electron-beam heated evaporated source

Figure 1 shows a schematic of the experimental arrangement. High rate evaporation of metal atoms is carried out using an electron beam to heat a pool of metal in the source in a vacuum chamber. A gas bleed is present to supply gas atoms for the reaction. The glow discharge is produced by having a probe in the experimental area to which a positive d.c. or even a.c. voltage is applied. When the voltage exceeds the breakdown voltage, e.g., 60 volts approximately or above for gas at pressure of 10^{-4} torr, a glow discharge is set up. The electrons in the electron beam are a key ingredient for the glow discharge also. In other words, the electron beam serves two functions: one, to heat the molten pool to evaporate metal atoms and two, to supply electrons for the glow discharge.
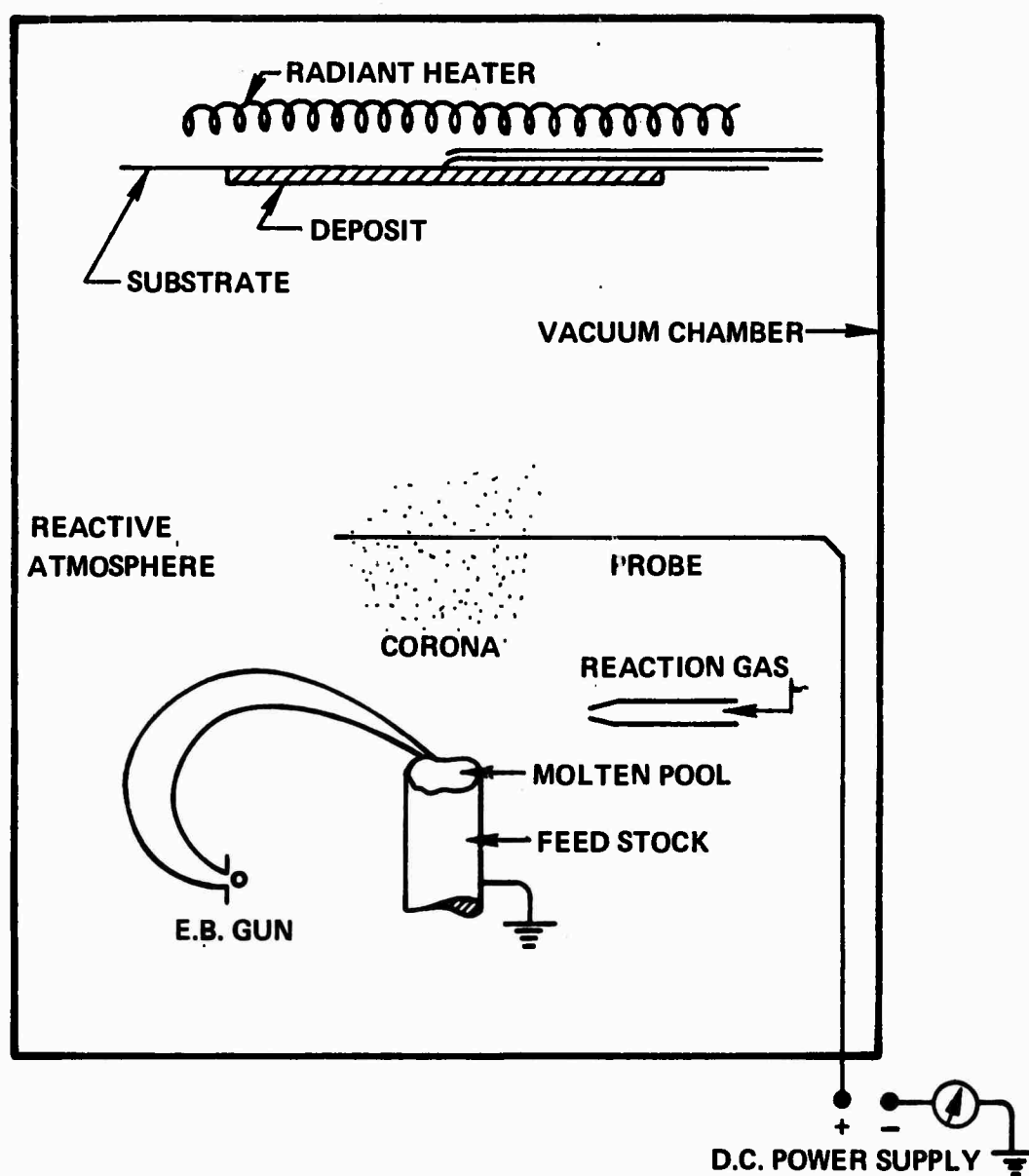
Figure 1. Activated Reactive Evaporation Under an Electrical Discharge.

The obvious fact which is not excluded is that if one uses another type of evaporation source (e.g., laser heated source) one would then provide a source of electrons or other conventional means to maintain a discharge.

A by-product of the process is that high purity compounds can be synthesized because the background impurity level in the gas phase is very low since one uses a vacuum environment, high purity metal and gas.

IV. Experimental set-up and procedure

A. Apparatus:

1. Vacuum system: The experiments were carried out in a conventional high vacuum system. The evaporation chamber is a 24 inch diameter and 36 inch high water-cooled stainless steel bell jar. The chamber is pumped by a 10 inch diameter fractionating diffusion pump, with an anti-migration type liquid nitrogen trap.

2. Electron beam source: The evaporation source is an one inch diameter rod fed electron beam gun - self-accelerated 270° deflection type- (Airco Temescal Model RIH-270) as shown in figure 2. The power supply for the gun is an Airco-Temescal (Model CV 30) 30 KW maximum power, operating at a constant voltage of 10 KV and variable emission current.

3. Substrate and substrate heater: The substrate is positioned 8 inches above the molten pool. The substrate is heated from behind by radiation from a 4 KW tungsten resistance heater. The temperature of the substrate is continuously recorded through a chromel-alumel thermocouple, which is spot welded at the center of the substrate on the back side as shown in figure 2. A movable shutter is located between the molten pool and the substrate.

1. Cathode Emitter, at -10kv
2. Electron Beam
3. Focus Magnet
4. Water-Cool Copper Crucible
5. Source Material
6. Copper Shielding
7. Shutter
8. Substrate
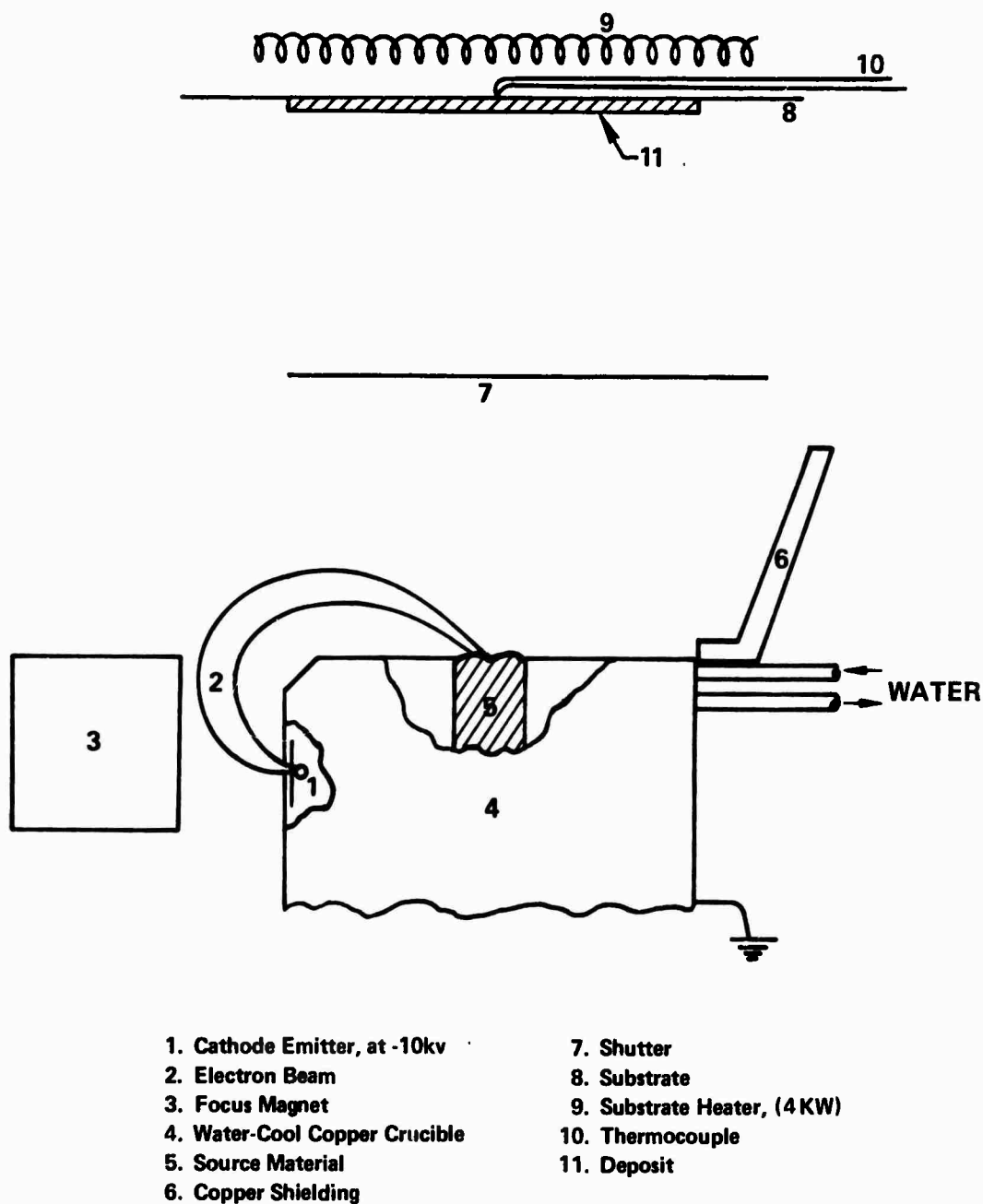9. Substrate Heater, (4 KW)
10. Thermocouple
11. Deposit

Figure 2. Schematic of Physical Vapor Deposition Process Using a Rod-Fed Source.

4. Substrate material: The deposits were collected on 5 mil thick stainless steel or copper substrates. A typical size of the substrate is 6" x 6" square. In few cases 5-6 mil thick titanium and zirconium substrates were also used.

5. Evaporant: the evaporants used in these series of experiments are: Ti, Zr, Hf, V, Nb, Si and Y. These evaporants were in the form of billets of 0.975 inch diameter and 6 inch maximum length.

6. Reactive gas bleed: The reactive gases were introduced into the chamber through a series of needle valves. The reaction gas pressures varied from 8×10^{-5} torr to 8×10^{-4} torr. The reaction gases used were commercial purity methane and acetylene for the synthesis of carbides, nitrogen and ammonia gases for the synthesis of nitrides and oxygen for the synthesis of oxides.

7. Power supply for the activated reactive evaporation: For activated reactive evaporation, the reactive gas molecules and/or the metal atoms from the pool were activated by a probe positioned between the pool and the substrate. An external a.c. with a line voltage of 110V or positive d.c. variable voltage was applied across the molten pool and the probe. The experimental arrangement for the activated reactive evaporation is shown in figure 1. The d.c. power supply used was a continuously variable voltage up to 500 V and 200 mA current, Lambda, Model 71.

B. Procedure:

The system was initially pumped down to 10^{-6} torr pressure range. Then the reaction chamber was purged with the reaction gas to 10^{-4} torr pressure range for few minutes and again the chamber is pumped down to 10^{-6} torr range before turning the electron beam on. This procedure is to make sure that the presence of extraneous gases is minimized.

When the pressure in the chamber went into the 10^{-6} torr range, the e.b. gun was turned on and the molten pool was formed with the shutter in the closed position. After forming the molten pool, the reaction gas was introduced into the chamber through the needle valve to get the required chamber pressure. For activated reactive evaporation the d.c. power supply was turned on and the potential was increased until a steady glow discharge was observed in the chamber. Once the steady glow had been set-in, the shutter was opened to deposit the compound on to the substrate.

C. Characterization of the synthesized compounds:

    1. X-ray analysis: The synthesized deposits were identified by their X-ray diffraction patterns. X-ray diffraction analysis was made on a G.E. XRD-5 diffraction unit using copper-K_α radiation with a nickel filter. For accurate determination of the lattice parameter, the unit was alligned using a standard tungsten specimen. The lattice parameters were determined by the method of least squares with 6 to 10 peaks depending on the deposit. From these lattice parameter measurements, the carbon to metal ratio, [C/M], in the carbides were determined using the published data on lattice parameters vs. [C/M] ratio.

    2. Microhardness measurements: Microhardness measurements of the deposits were made using a Kentron microhardness tester, with a diamond pyramid indentor. A load of 50 g was used in all cases. The diagonal length of the indentations varied from 5.7μm to 9.0μm and about 1μm in depth. In each case an average of four indentations were made. There was a considerable scatter in the results, and the maximum scatter was about 10% of the measured value.

V. Results and Discussion

A. Voltage-current characteristics of activated reactive evaporation:

A glow discharge voltage and current varied over a wide range depending on the reactive gas, position and area of the probe and the electron beam gun emission current. Typical voltage - current characteristic curves are shown in figure 3 for molten Ti pool at various beam currents and two acetylene pressures. When the glow discharge sets-in the chamber, a colored glow was observed inside the chamber and the discharge current drastically increased as illustrated in figure 3.

With higher beam currents, the potential required for initiating the glow discharge decreases. Once glow discharge sets in, the current in the probe increases rapidly. Increase in the surface area of the probe increased the glow discharge current and decreased the voltage required for the glow discharge. Typically for titanium, the voltage required for a glow discharge was in the range of 60 to 90 volts, at $p_{C_2H_2}$ = 1 to 3.10^{-4} torr with tungsten wire of diameter and length 1.25 mm, 50 mm.

It has long been known that chemical reactions can occur in gases which are subjected to electrical stresses. One of the earliest commercial uses was the application of a high voltage corona discharge in oxygen to form ozone.[15] In spite of its early use of corona discharges for promoting chemical reactions, the exact mechanism is not well understood.[16] In the present context, a few possible effects of the glow discharge could be; (i) glow discharge may increase the temperature of the glow region which promotes the chemical reaction, (ii) glow discharge may ionize the metal atoms and/or the gas molecules, which increases their chemical reactivity, (iii) in the glow region the collision probability of the reacting species may be enhanced. The above factors may each contribute to a certain extent in promoting the overall chemical reaction. Detailed investigations are
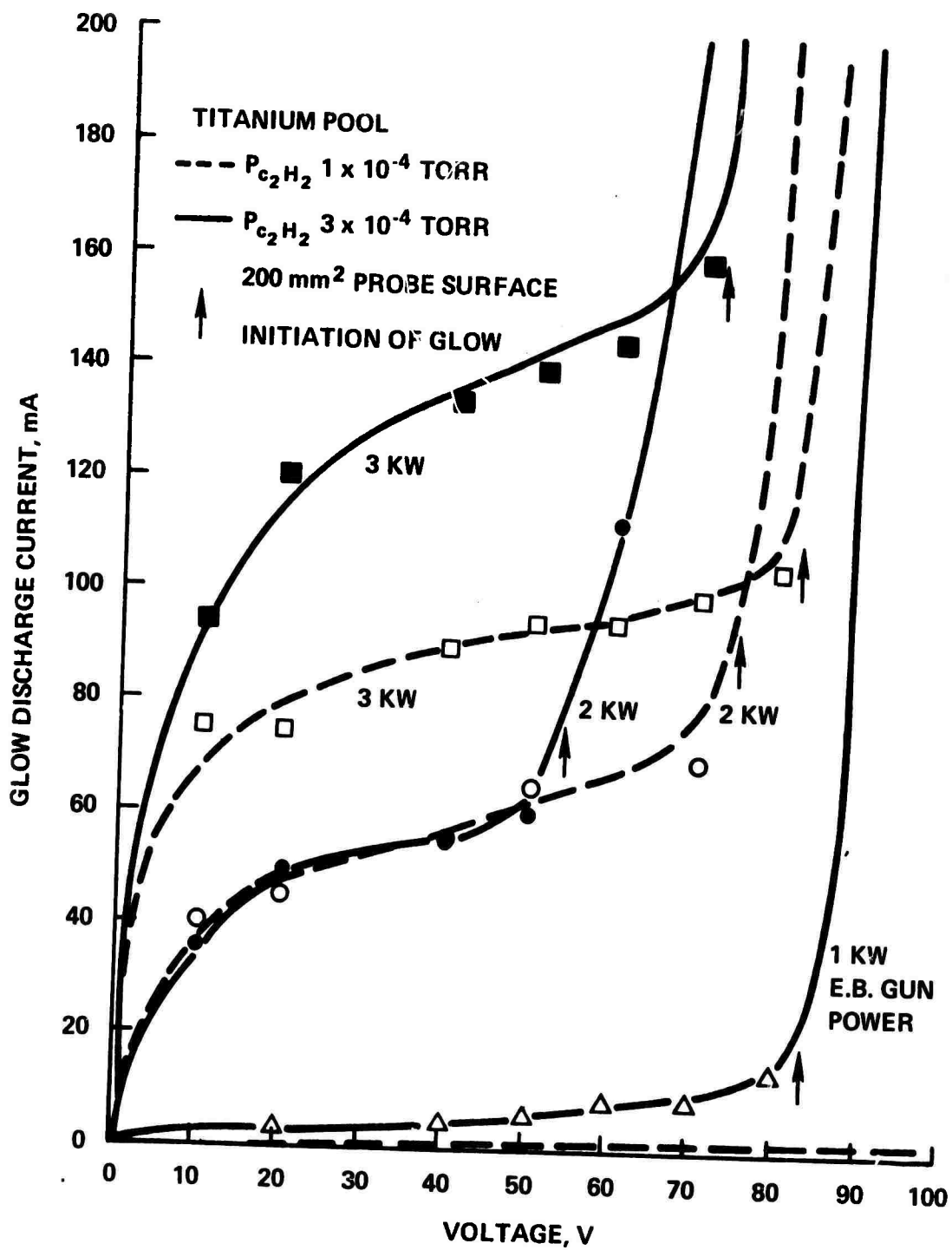
Figure 3. Variation of Glow Discharge Current With Voltage at Different C_2H_2 Pressures and Emission Currents for Titanium.

necessary for a complete understanding of the reaction mechanism in the glow discharge region.

B. Materials synthesized:

1. Oxides: Yttrium oxide is the only oxide synthesized so far by reactive evaporation with oxygen bleed and without the external potential. Yttrium oxide was also synthesized by activated reactive evaporation, with oxygen and an external potential. In both cases a red glow was observed in the chamber. Dense Y_2O_3 was deposited on stainless steel substrate at room temperature and at 790°C.

2. Carbides: Attempts were made to synthesize carbides, by reactive evaporation with methane and acetylene gases, but in both cases it was not possible to produce carbides. However, several carbides were synthesized by the activated reactive evaporation with acetylene gas as the reactive atmosphere. The carbides synthesized at the time of this report are TiC, ZrC, HfC, VC, NbC and SiC. The experimental conditions under which these carbides were synthesized are tabulated in table I. For carbide synthesis by activated reactive evaporation methane gas was also tried but no carbide was produced. This is probably due to the saturated carbon-hydrogen bond in methane. On the contrary, acetylene is a highly unsaturated hydrocarbon, which could be easily dissociated in the glow region. The deposition temperatures for carbides were varied from room temperature to about 700°C. The deposits made at room temperature were very loose and flaky; on the contrary deposits at higher substrate temperatures were dense and adhere well to the substrates.

3. Nitrides: Titanium nitride is the only nitride synthesized so far by reactive evaporation using nitrogen gas, at $p_{N_2} = 4.10^{-4}$ torr on stainless steel and copper substrates at room temperature. However, the

It was found that as the pressure of the reaction gas increases the [C/M] ratio also increases at a constant flux density of titanium atoms. From table III it can be seen that at $p_{C_2H_2} < 3.10^{-4}$ torr, the X-ray diffraction patterns of the deposit indicated the presence of both Ti and TiC phases. With $p_{C_2H_2} \geqslant 3.10^{-4}$ torr the [C/M] ratio increases with the reaction gas pressure from 0.6 to 1.0 at $p_{C_2H_2} \geqslant 5.10^{-4}$ torr for a rate of deposition of 4μm/min.

The rate of deposition of the carbide was varied by changing the rate of evaporation of titanium. The deposition rates of TiC was varied from 0.6μm/min to 10.0μm/min. At a constant $p_{C_2H_2}$ 4.10^{-4} torr, the increase in the rate of deposition up to 6.0 m/min decreased the [C/M] ratio in titanium carbide on a substrate at 8 inches from the pool. The results are listed in table IV. For TiC deposition at rates 8.0μm/min, at constant gas pressure of $p_{C_2H_2} = 4.10^{-4}$ torr, the deposits contained both Ti and TiC. Hence, for synthesizing stoichiometric composition of TiC, the flux density of titanium atoms and the pressure of acetelene gas should be optimized. For example, for a TiC deposition rate of 4.0 m/min and $p_{C_2H_2} = 5.10^{-4}$, the TiC deposit had a $TiC_{1.0}$ stoichiometry.

2. <u>Microhardness and the influence of oxygen on microhardness and lattice parameter</u>: Tables II, III, and IV also show the microhardness measurements of the carbides (at 50 g load). Microhardness values are very sensitive to the applied load[18] and vary markedly with the [C/M] ratio[17,19], oxygen content[20], and the structure of the deposit.[21] In table II the measured hardness values are compared with the published values. In the case of TiC, with [C/M] = 1.0, the measured hardness value of 2775 kg/mm^2 which was obtained by extrapolation to [C/M] = 1.0.[19]

nitride deposited by reactive evaporation at room temperature was loose and flaky and the x-ray diffraction pattern showed the existance of both Ti and TiN. Titanium nitride was also synthesized by activated reactive evaporation using nitrogen and ammonia gases, with the substrate at room temperatures. In both techniques the deposits made at higher substrate temperatures ($\sim$400°C) did not form the nitrides. The nitride deposited with activated nitrogen gas at p_{N_2} = 4.10^{-4} torr, did not indicate the presence of free titanium, unlike the nitride deposited by reactive evaporation at the same pressure of nitrogen. This illustrates the increase in reaction efficiency by the activation of the reacting species.

C. Characterization:

1. X-ray analysis and carbon to metal ratios in carbides: X-ray diffraction peaks for the carbides deposited at higher substrate temperatures were sharp and narrow, indicating the fine grain size and with no pronounced residual stresses. The diffraction patterns also showed varying degrees of preferred orientations.

The results of the lattice parameter measurements for the carbides are tabulated in table II. From these lattice parameters [C/M] ratios were estimated using the data tabulated by Pearson.[14] The carbon to metal ratios [C/M] in the carbides are greatly influenced by the various process variables. The important variables are the nature and partial pressures of the reactive gases in the reaction chamber, rate of evaporation of the metal from the pool, the substrate material and its temperature.

The synthesis of TiC was studied in some detail, i.e., the variation in [C/M] ratio with acetylene gas pressure and the rate of deposition. The results are tabulated in tables III and IV.

Both measurements were made with diamond pyramid indentor at 50 g load.
In the case of ZrC, HfC and VC, the published values appear to be higher,
but the direct comparison with the measured values are not meaningful.
For ZrC[22] and VC,[23] the loads used were not specified. For HfC[24]
the reported value is measured with the Knoop indentor using 100 g load,
a direct comparison is not possible. Microhardness measurements, especially
for very high hardness values at low loads, are very strongly influenced
by the applied load; e.g., in the case of $TaC_{0.83}$, with 100 g load, the
hardness reported was 2400 Kg/mm^2 and with 25 g load the hardness reported
in the same work was 3000 kg/mm^2.[25]

The presence of oxygen in carbides is known to increase the microhardness
values.[20] This may also contribute to the low hardness values reported
in the present series of experiments, where the technique permits the
synthesis of carbides which minimizes the possibility of oxygen contamina-
tion.

Further evidence of low oxygen content in the carbides synthesized
in this investigation can be deduced from lattice parameter measurements.
The lattice parameters measured for $TiC_{1.0}$ and $VC_{1.0}$ are higher than the
published values of lattice parameter,[26] as illustrated for TiC in
Figure 4. The published values of lattice parameters vs. [C/M] ratio for
TiC, ZrC, VC show increasing lattice parameters going through a maximum
and then decreasing as the [C/M] ratio approaches 1.0.[17] According to
Vegard's Law, the lattice parameter should have increased linearly with
[C/M] ratio. This falling off of the lattice parameter which is a devia-
tion from Vegard's Law has been attributed to the presence of oxygen.[17]
In the present case with TiC, the low oxygen content might account for the
absence of a maximum, with the lattice parameter constantly increasing in
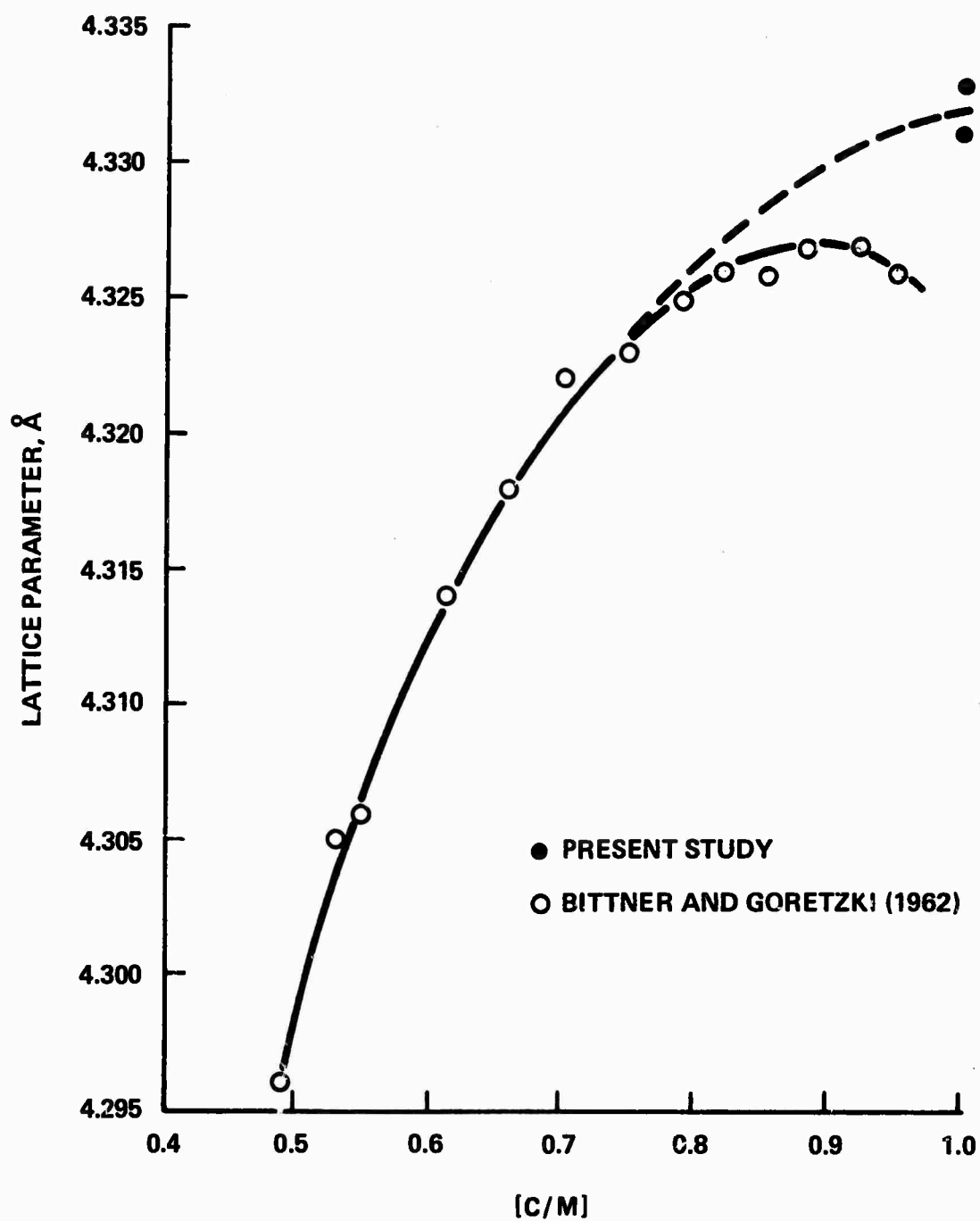accordance with Vegard's Law, as shown in Figure 4. Therefore, the high

Figure 4. Lattice Parameter of TiC as a Function of [C/M] Ratio.

lattice parameter values and the low microhardness values may be due to the very low oxygen content. Chemical analysis of the carbides for combined carbon, free carbon and oxygen content will be carried out to test these results.

D. Deposition rates:

In reactive evaporation as well as in activated reactive evaporation, the deposition rate is influenced by the flux density of metal atoms, the pressure of the reacting gas, the collision frequency between metal and gas atoms and the reaction efficiency. The last two factors are higher in activated reactive evaporation than in reactive evaporation. The stoichiometry of the compound depends on the number of metal atoms and gas atoms. The overall deposition rate can therefore be increased by increasing these quantities provided the reaction efficiency does not decrease. In activated reactive evaporation, there is an experimental parameter which also has a bearing on this matter, i.e., the current drawn by the probe which is limited by the current carrying capacity of the glow discharge power supply. In this investigation, the supply had a maximum current limitation of 200 ma which limited the gas pressure that could be used. Hence, for synthesizing a $TiC_{1.0}$ stoichiometry, these interrelated factors resulted in the following experimental parameters — for TiC, the rate of deposition of $4\mu m/min$ and $P_{C_2H_2} = 5.10^{-4}$ torr was found to produce a carbide having $TiC_{1.0}$ stoichiometry.

In the future, we plan to use a power supply with 1.5 amps maximum current capability and hence expect to go to higher deposition rates. Another experimental problem can be the high pressure operating limit of 1.10^{-3} torr for thermionically excited electron beam guns. This can be easily overcome by separate pumping of the emitter section of the gun.

VI. Summary and Conclusions

Synthesis of compounds was carried out by reactive evaporation. In reactive evaporation, the metal atoms are evaporated from a source in the presence of a reactive gas atmosphere so as to form a compound. Yttrium oxide and titanium nitride have been synthesized by the reactive evaporation using oxygen and nitrogen gases as reactive atmospheres respectively. However, attempts to synthesize titanium carbide by reactive evaporation using methane and acetylene gases were not successful.

A new technique of Activated Reactive Evaporation has been developed and successfully used for synthesis of carbides as well as oxides and nitrides. In activated reactive evaporation the reacting species are activated by the glow discharge initiated in the reaction zone. This technique when used with an electron beam evaporation source, with the electrons from the e.b. gun also being used for the glow discharge, thus creates the discharge right in the reaction zone where it is needed for maximum reaction efficiency.

This technique has several advantages for the synthesis of compounds. They are: (i) very high deposition rates of up to $10.0 \mu m/min$, which is an order of magnitude higher than known processes, such as chemical vapor deposition, sputtering, etc. (ii) lower substrate temperatures ($\sim 400°C$) can be used for obtaining full density deposits as compared to substrate temperature, $> 1000°C$ for chemical vapor deposition. (iii) it is possible to synthesize high purity compounds, with controlled stoichiometry.

This technique has also been used successfully for synthesis of Y_2O_3 with oxygen as the reaction gas, and TiN with nitrogen and ammonia as reaction gases. For TiN with nitrogen as reaction gas, it was found that reaction efficiency increased using activated reaction evaporation as compared to reactive evaporation.

For the first time carbides of group IV and V metals have been synthe-sized by physical vapor deposition processes using activated reactive evap-oration with acetylene as the reactive gas. [C/M] ratios in the carbides were varied by varying the rate of evaporation of the metal and the pressure of the reaction gas. For titanium carbides, an optimum rate of deposition of 4.0μm/min and $p_{C_2H_2} = 5.10^{-4}$ torr was found to produce a carbide having a stoichiometry $TiC_{1.0}$ and microhardness of 2775 kg/mm^2. Higher deposition rates can be achieved by increasing the current carrying capacity of the glow discharge power supply and the reaction gas pressures.

References

1. Brinsmaid, S., Keenan, W. J., Koch, G. E., and Parsons, W. F.,
    U.S. Patent 2,784,115 March 5, 1957.

2. Auwarter, M., U.S. Patent 2,920,002 January 5, 1960.

3. Herrick, C. S., and Tevebaugh, A. D., J. Electrochem. Soc., 110,
    119, (1963).

4. Novice, M. A., Bennett, J. A., and Cross, K. B., Eleventh Vacuum
    Symposium Abstracts, J. Vac. Soc. Tech. 1, 73A (1964).

5. Schilling, R. B., Proc. IEEE 52, 1350 (1964).

6. Ritter, E., J. Vac. Sci. Tech., 3, 225 (1966).

7. Rairden, J. R., Electrochem. Tech. 6, 269 (1968).

8. Rairden, J. R., "Thin Film Dielectrics," Ed. F. Vratny, Electrochem.
    Soc., N. Y., 279 (1969).

9. Ferrien, E., and Pruniaux, B., J. Electrochem. Soc., 116, 1008 (1969).

10. Learn, A. J., and Haq, K. E., Appl. Phys. Letters, 17, 26 (1970).

11. Bunshah, R. F. Patent Disclosure, November 1970.

12. Wank, M. T., and Winslow, D. K., Appl. Phys. Letters, 13, 286 (1968).

13. Kosicki, B. B., and Khang, D., J. Vac. Sci. Tech. 6, 592 (1969).

14. Pearson, W. P., "A Handbook of Lattice Spacings and Structure of
    Metals and Alloys" Vol. 2, Pergamon Press, N. Y. (1967).

15. Warburg, E., and Rumpf, W., Z. Phys. 32, 245 (1925).

16. Kondratev, V. N., "Kinetics of Chemical Gas Reactions" Book 2, Academy
    of Science, USSR, Moscow, (1958).

17. Storms, E. K., "The Refractory Carbides," Academic Press, N. Y. (1967).

18. Buckle, H., Met. Rev., 4, 49 (1959).

19. Williams, W. S., and Lye, R. G., ML-TDR-64-25, Air Force Materials
    Laboratory, Research and Technology Div., Air Force Systems Command,
    Wright Patterson AFB, Ohio; cited in Ref. 17.

20. Cadoff, I., Nielsen, J. P., and Miller, E., Plansee Proc., 2nd Seminar
    Reutte/Tyrol, Pergamon Press, Oxford, 50 (1955).

21. Movchan, B. A., and Demchishin, A. V., Fiz. Metalloved., 28, 653 (1969)

22. Koval'skii, A. E., and Makavenko, T. G., Trans. Conf. Microhardness, Academy of Sciences, USSR, Moscow, 187 (1951).

23. Gurevich, M. A., and Ormont, B. F., Zh. Veorgan. Khim. $\underline{7}$, 1566 (1957).

24. Adams, R. P., and Beall, R. A., BM-RI-6304, Bureau of Mines, Reports of Investigations, (1963).

25. Santoro, G. J., Trans. AIME, $\underline{227}$, 1361 (1963).

26. Bittner, H., and Goretzki, H., Monatsh. Chem. $\underline{93}$, 1000 (1962).

List of Tables

List of Figures

TABLE I

Experimental Conditions for the Reactive and
Activated Reactive Evaporation of Compounds

Run #	Reactive Atmosphere		$T_{substrate}$ °0	Rate of deposition $\mu m/min$	Remarks
	P_{gas} torr	w or w/o potential			
$Y-0_2-2$	1.10^{-4}	w/o potential	Room temp.	13.0	
$Ti-N_2-9$	4.10^{-4}	"	"		Ti+TiN
$Ti-N_2-8$	4.10^{-4}	w/ potential	"		
$Ti-NH_3-2$	4.10^{-4}	"	"		
$Ti-C_2H_2-34$	5.10^{-4}	"	450	4.0	
$Zr-C_2H_2-1$	4.10^{-4}	"	540	5.0	
$Hf-C_2H_2-2$	4.10^{-4}	"	515	2.5	
$V-C_2H_2-5$	5.10^{-4}	"	555	3.0	
$Nb-C_2H_2-2$	4.10^{-4}	"	540	2.5	
$Si-C_2H_2-1$	4.10^{-4}	"	690	0.8	Si+SiC

TABLE II

[C/M] Ratios and Microhardness of Carbides
of Group IV and V Metals

Run #	Carbide	Lattice Parameter $\overset{\circ}{A}$	$[\frac{C}{M}]$	Microhardness, Kg/mm^2 Present 50 g load	Published Values
Ti-C$_2$H$_2$-34	TiC	4.3283	1.0	2775	2900[a]
Zr-C$_2$H$_2$-1	ZrC	4.7061	.9	1150	2500[b]
Hf-C$_2$H$_2$-2	HfC	4.6562	1.0*	1580	2276[c] (KHN)
V-C$_2$H$_2$-5	VC	4.1840	1.0	1924	3000[d]
Nb-C$_2$H$_2$-2	NbC	4.4287	.7*	1700	—

*The starting materials Hf and Nb were not pure. Hf was a crystal bar and
Nb was a low alloy billet.

a. DPHN, Load 50g, values extrapolated to [C/M] = 1.0[19]

b. DPHN, Load not specified, [C/M] = 0.9[22]

c. KHN, Load 100g, [C/M] = 1.0[24]

d. DPHN, Load not specified, [C/M] = 1.0[23]

TABLE III

Variation of [C/M] Ratio and Microhardness
with Pressure of Reaction Gas for TiC

Run #	$P_{C_2H_2}$ torr	Rate of deposition μm/min	Lattice Parameter Å	$[\frac{C}{M}]$	Microhardness 50 g load Kg/mm^2
Ti-C$_2$H$_2$-34	1.10^{-4}	4	-	Ti+TiC	-
Ti-C$_2$H$_2$-34	3.10^{-4}	4	4.3119	0.6	2,000
Ti-C$_2$H$_2$-35	4.10^{-4}	4	4.3229	0.75	2,550
Ti-C$_2$H$_2$-34	5.10^{-4}	4	4.3283	1.0	2,775
Ti-C$_2$H$_2$-34	$7-8.10^{-4}$	4	4.3312	1.0	2,670

TABLE IV

Variation of [C/M] Ratio and Microhardness
with Rate of Deposition for TiC

Run #	$P_{C_2H_2}$ torr	Rate of Deposition m/min	Lattice Parameter Å	$[\frac{C}{M}]$	Microhardness 50 g load kg/mm^2
Ti-C$_2$H$_2$-35	4.10^{-4}	0.6	-	-	-
Ti-C$_2$H$_2$-35	4.10^{-4}	3.0	4.3273	.9	-
Ti-C$_2$H$_2$-35	4.10^{-4}	4.0	4.3229	.75	2550
Ti- C$_2$H$_2$-35	4.10^{-4}	6.0	4.3108	.6	2070
Ti-C$_2$H$_2$-35	4.10^{-4}	8.0	-	Ti+TiC	-
Ti-C$_2$H$_2$-35	4.10^{-4}	9.7	-	Ti+TiC	-

PART II

THE PROPERTIES OF RARE EARTH METALS AND ALLOYS
TASK IV

D. L. Douglass

Introduction

The presence of small amounts of certain rare earth elements in nickel-base alloys is known to markedly reduce the rate of oxidation at high temperatures and to exert a highly beneficial effect on the mechanical stability of the scales formed. The effect is disproportionate to the amount added. General a fraction of a percent, e.g., approximately 0.1 to 0.3%, is suf ient. In particular, the resistance to exfoliation of the scales beco s outstanding.

The mechanism by which these effects occur is not known and has been subject to rather wild speculation. The program in progress is directed at obtaining an understanding of the mechanism and to characterize the oxidation behavior of certain alloys containing rare earth additions.

Results

Oxidation Kinetics

Isothermal oxidation was performed over the range of 900 to 1200°C as described in the first Semi-Annual Technical Report.[1] All samples were initially weighed and oxidized for 1 hour at the temperature of interest. They were subsequently reweighed and inserted in the Harrop GTA unit which was slowly heated to the oxidation temperature; no changes occurred during the heating when the samples had been preoxidized. The difference in the oxidation rate may be seen in Figure 1., which shows an approximate fit to the cubic rate law and the slowly heated sample oxidizing more rapidly by a factor of about 10% than the sample immersed directly. This difference is related to the nature of the oxide film formed at low temperatures, e.g., during slow

heating, compared to the films formed at high temperatures, e.g.,
immersed directly. Figure 2 shows a comparison of X-ray diffraction
patterns taken from the two samples, and Figure 3 is a composite of
X-ray images obtained by the electron microprobe. Basically, the
slowly heated sample contains a much higher fraction of NiO in the
film compared to the sample immersed directly which has a film consis-
ting primarily of Cr_2O_3. Some spinel also exists, having formed
by the reaction of NiO with Cr_2O_3. The latter forms by either internal
oxidation of the chromium-enriched substrated surface or by a displace-
ment reaction in which chromium reduces NiO. These will be discussed
in more detail subsequently. The important point for the moment is
that differences do exist depending upon the way the test is carried
out and that these differences are readily explained by the consti-
tuents of the films formed.

Effect of Rare Earth Additions

The isothermal oxidation curves for all four alloys, Ni-20Cr
and Ni-20Cr containing nominally 1% of Gd, La, and Y are presented
in Figures 4-6 for temperatures of 1000, 1100, and 1200°C, respectively.
The presence of the rare earths reduced the oxidation rate of the
pure alloy at all temperatures. The weight gain followed a time law
which was approximately cubic, e.g., $\Delta w = kt^{1/3}$, although some of
the alloys exhibited less than the cubic rate law and the rates generally
decreased with time. Yttrium was the most effective addition at all
temperatures, the extent of the reduction in rate being about a factor
of five. Gadolinium was more effective than lanthanum in reducing the
oxidation rate at temperatures in the range of 900 to 1100°C, but at
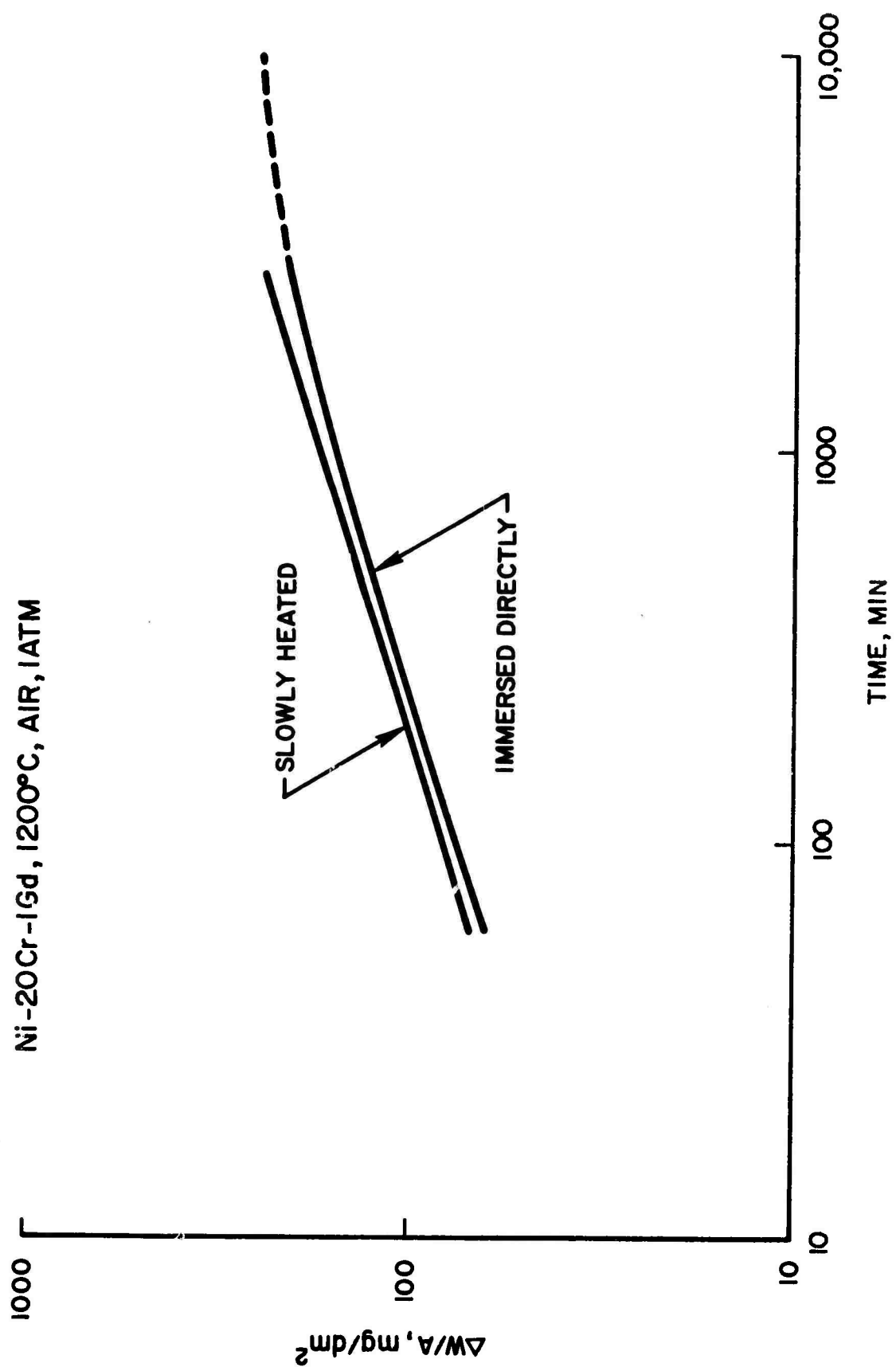1200°C, the reverse was true.

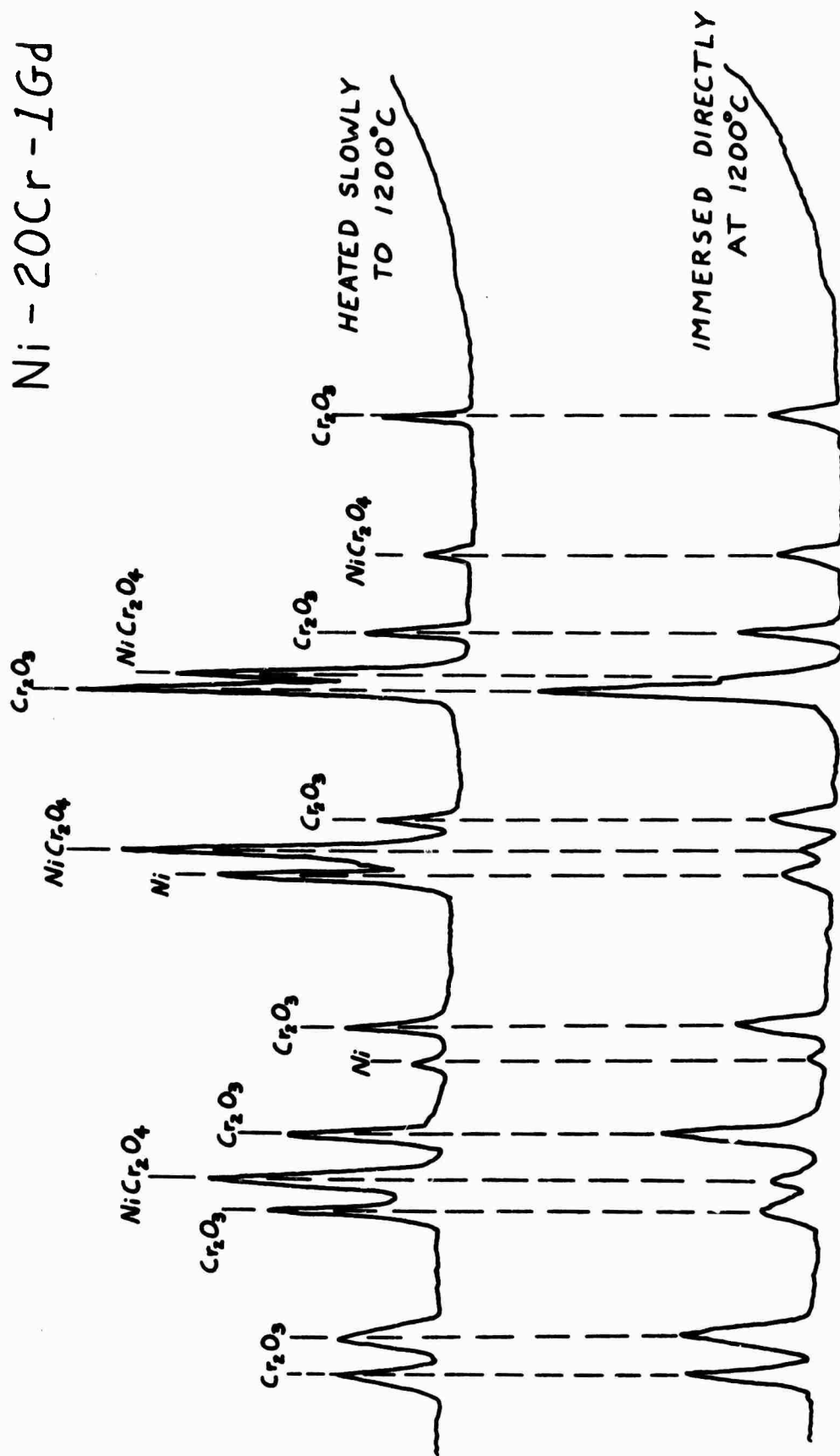Figure 1.   Effect of Testing Method on the Oxidation Kinetics of Ni-20Cr-1Gd.

Ni - 20Cr - 1Gd

Figure 2.   Comparison of X-Ray Diffraction Patterns of Oxide Scales Formed on Samples in Figure 1.

BACK-SCATTERED
ELECTRONS

Cr

Ni

Gd

⊢
10μ

SLOWLY HEATED TO
1200°C

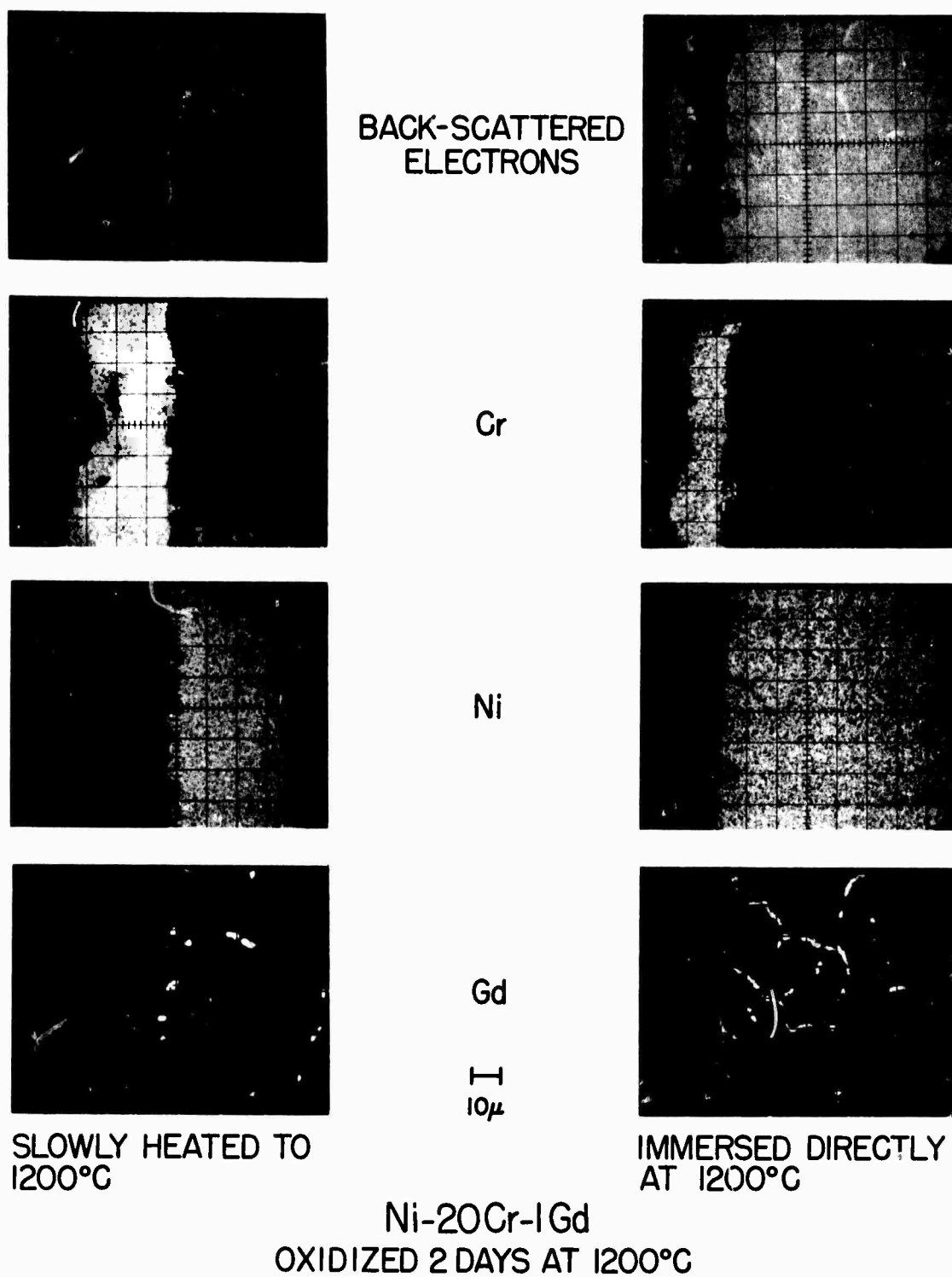IMMERSED DIRECTLY
AT 1200°C

Ni-20Cr-1Gd
OXIDIZED 2 DAYS AT 1200°C

Figure 3.   Comparison of Electron Microprobe Analyses of Oxide Scales Formed on Samples in Figure 1.
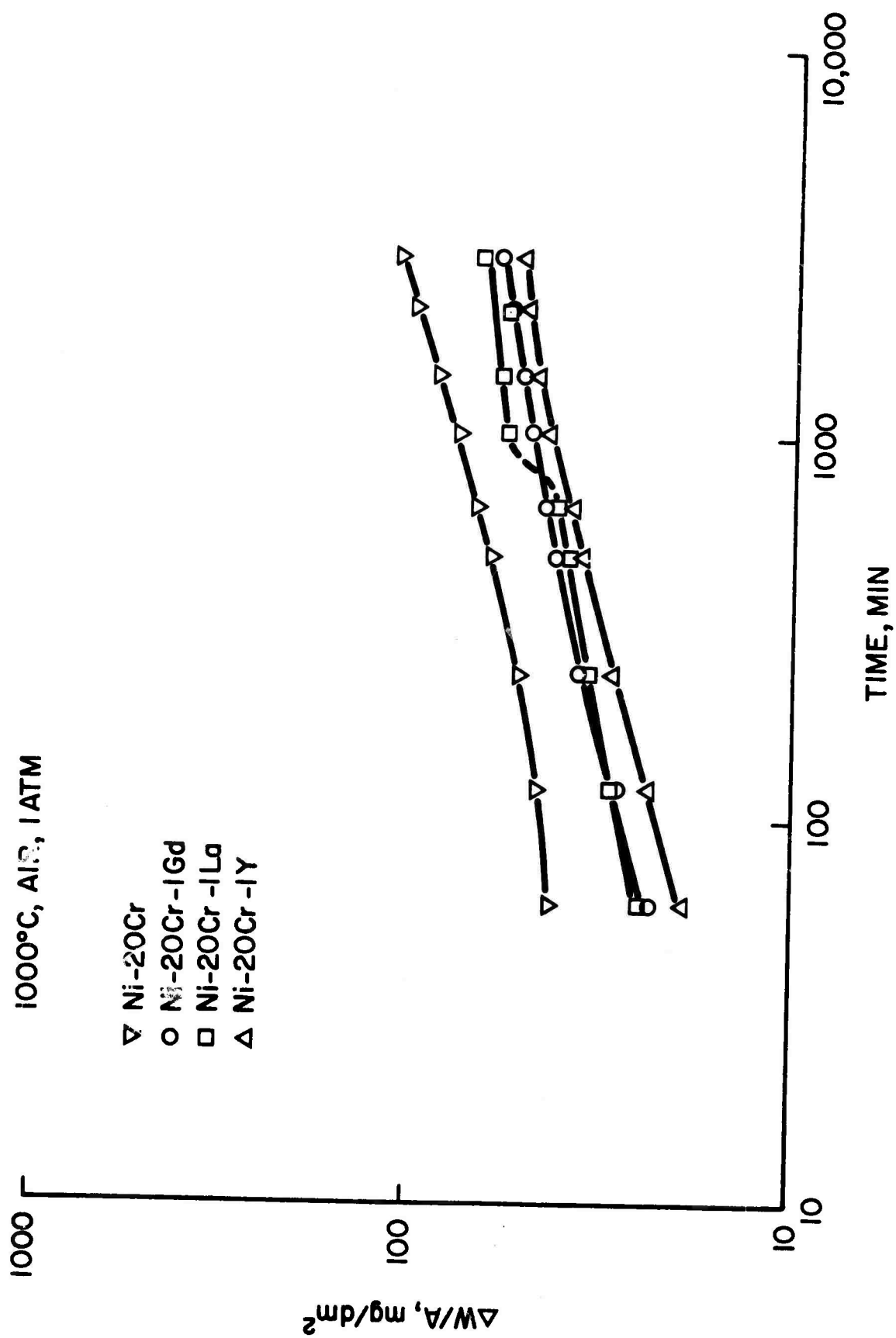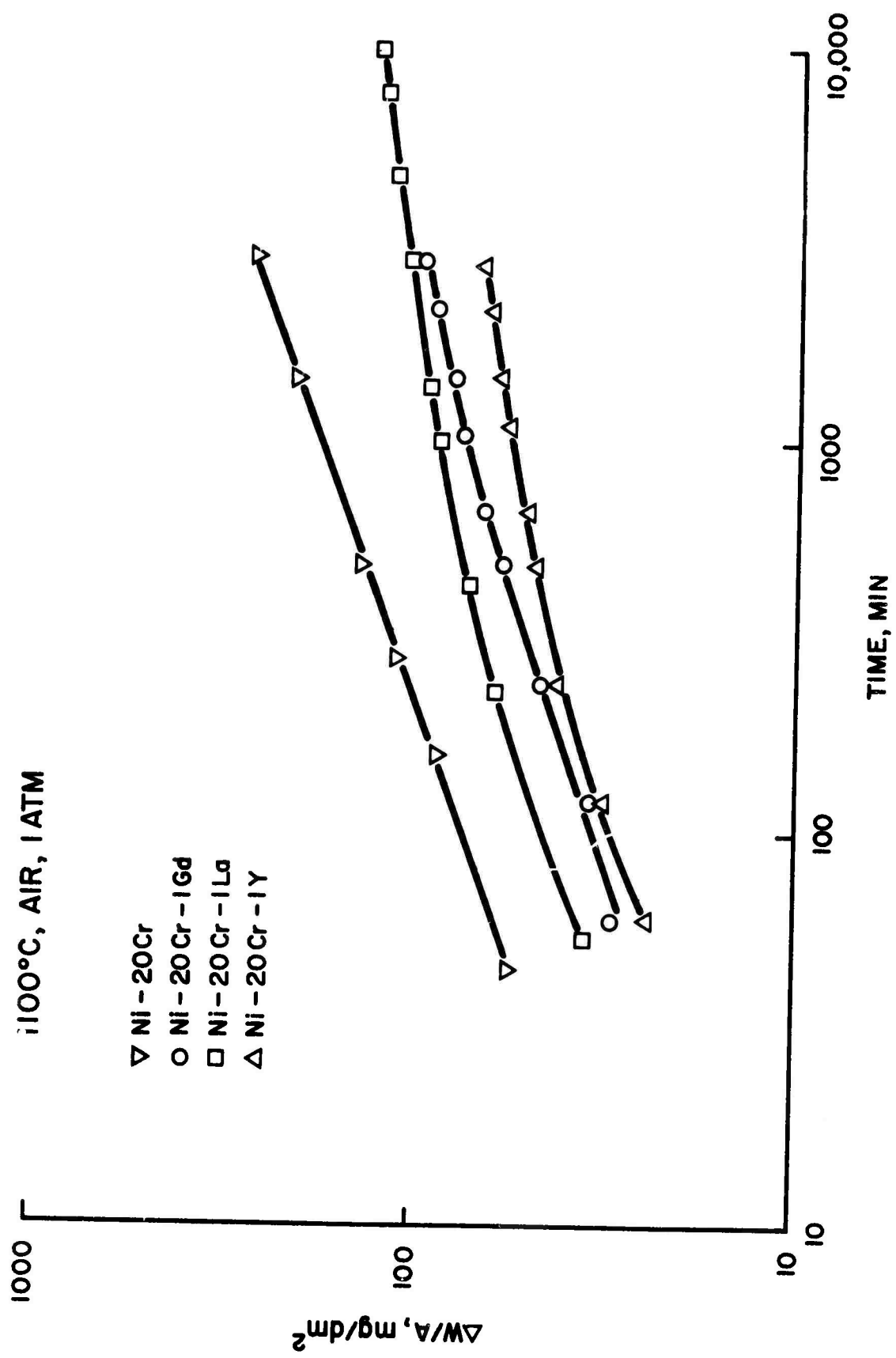
Figure 4. Oxidation Kinetics of Alloys Tested at 1000°C.
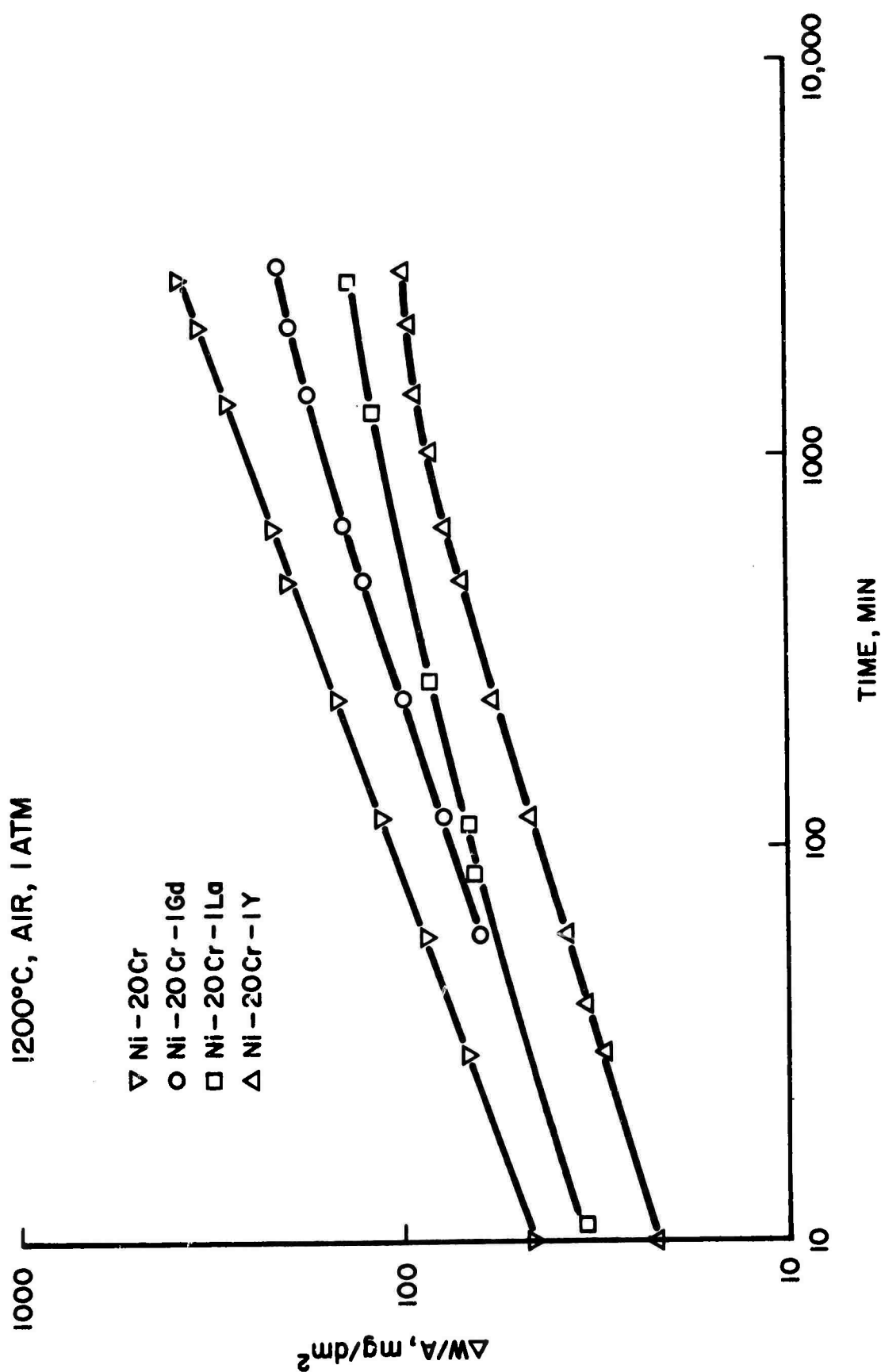
45

Figure 5.   Oxidation Kinetics of Alloys Tested at 1100°C.

1100°C, AIR, 1 ATM

▽ Ni – 20Cr
○ Ni – 20Cr – 1Gd
□ Ni – 20Cr – 1La
△ Ni – 20Cr – 1Y

TIME, MIN

ΔW/A, mg/dm²

Figure 6. Oxidation Kinetics of Alloys Tested at 1200°C.

The temperature dependence of the oxidation is shown in Figure 7 which is an Arrhenius plot of log reciprocal time* to achieve an arbitrary weight gain (50 mg/dm^2) versus reciprocal temperature. There is no physical meaning to this plot in the sense that a fundamental law applies and that activation energies might be compared to various physical processes. This plot is a convenient way in which the temperature dependence of oxidation may be shown for the alloys and the alloys compared to one another. The complex nature of the scales and the fact that no particular time law was followed by all alloys over the complete time period studied precludes a detailed analysis of the Arrhenius plot. It is clear, however, that the rare earths do indeed reduce the oxidation rate, and that yttrium is by far the most effective.

Structure of Oxide Scales

X-ray diffraction and electron microprobe analyses of scales were made using standard techniques. Preparation of metallographic samples (used for the microprobe) was quite difficult due to loss of the scale by mechanical failure during mounting and grinding. This problem was finally solved by vapor plating with a thin layer of gold in vacuum (to make the samples conducting) followed by an electroplating of copper to a thickness of about 0.002 to 0.004." The plated samples could then be subjected to careful grinding and polishing.

---

*
reciprocal times were used because they have the same units as a rate and give the correct slope of log rate versus reciprocal temperature on an Arrhenius plot.
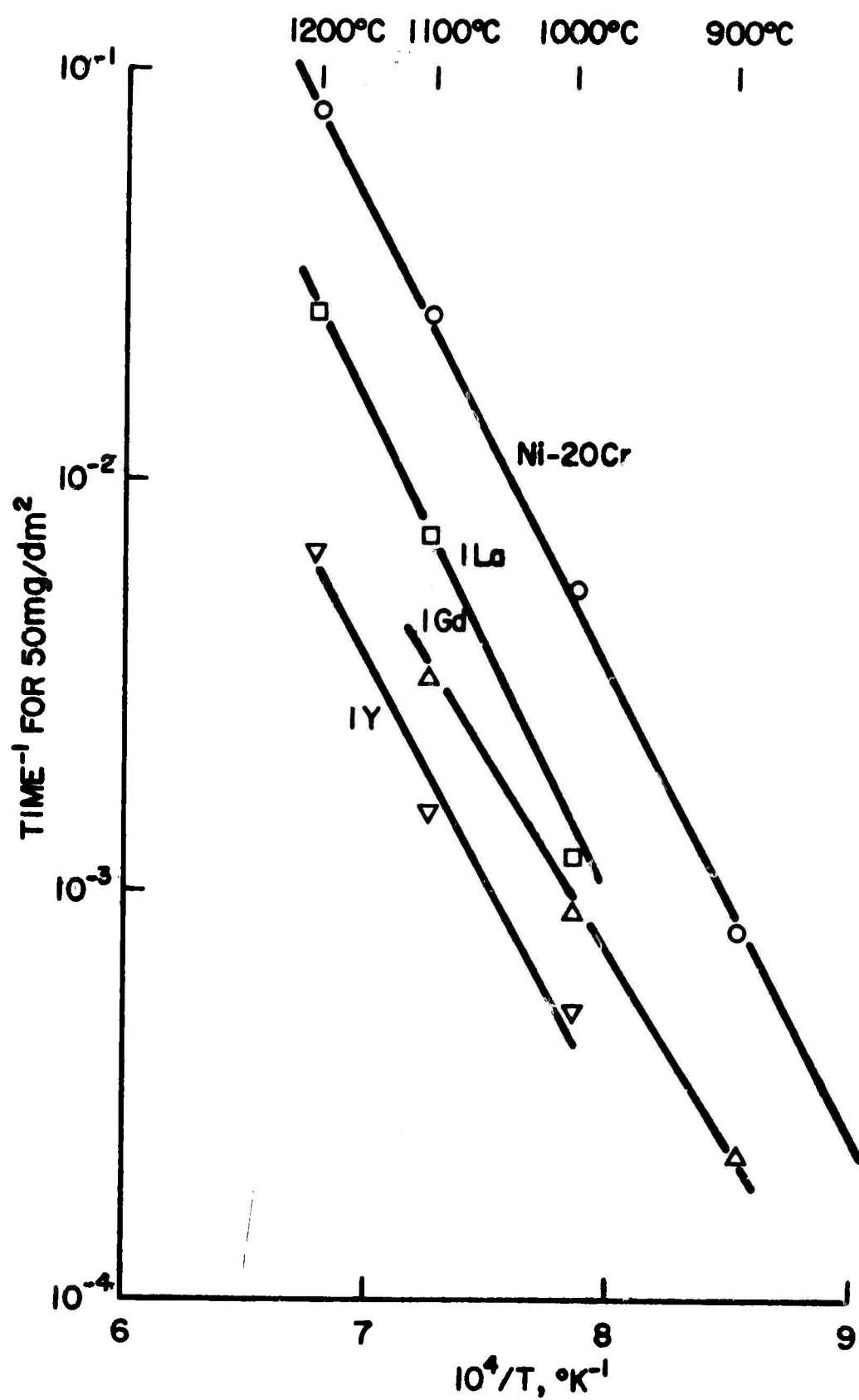
Figure 7.   Arrhenius Plot Showing Temperature Dependency of Oxidation Rates.

X-ray diffraction scans are shown in Figs. 8-11 for each alloy. The figures include both "low" and "high"-temperature scales. In general, the "low"-temperature scales contain much NiO and spinel with lesser amounts of Cr_2O_3. The "high"-temperature scales were primarily Cr_2O_3 with some spinel and very little if any NiO. There was no evidence of any rare earth oxides or mixed oxides containing rare earths with the exception of the alloy containing yttrium oxidized at 1200°C. One diffraction line could be indexed as Y_2O_3. However, as will be seen from the probe results, this could be attributed to Y_2O_3 existing in the substrate grain boundaries.

Electron microprobe results are shown in Figures 12-15. The scales are primarily Cr_2O_3 at the "high" temperature, e.g., 1100 or 1200°C, with a small amount of spinel at the oxide/gas interface. The "low"-temperature scales contained an appreciable fraction of Cr_2O_3, but they also showed substantial amounts of NiO at the exterior. The only evidence of any rare earth in the scales was on the Ni-20Cr-1Y alloy oxidized at 1200°C. A thin layer of a Y-rich phase was detected at the oxide/gas interface. All of the rare earths existed as oxides in the substrate grain boundaries as can be clearly seen from the X-ray images for the rare earths. Although oxygen images are not shown, they were run on several samples and showed unequivocally that the rare earths existed as oxides in the grain boundaries. This was in contrast to the existence of rare earth-nickel intermetallic compounds dispersed throughout the alloy matrix away from the oxide/metal interface. It thus appears that the rare earth-nickel intermetallics were preferentially oxidized internally.
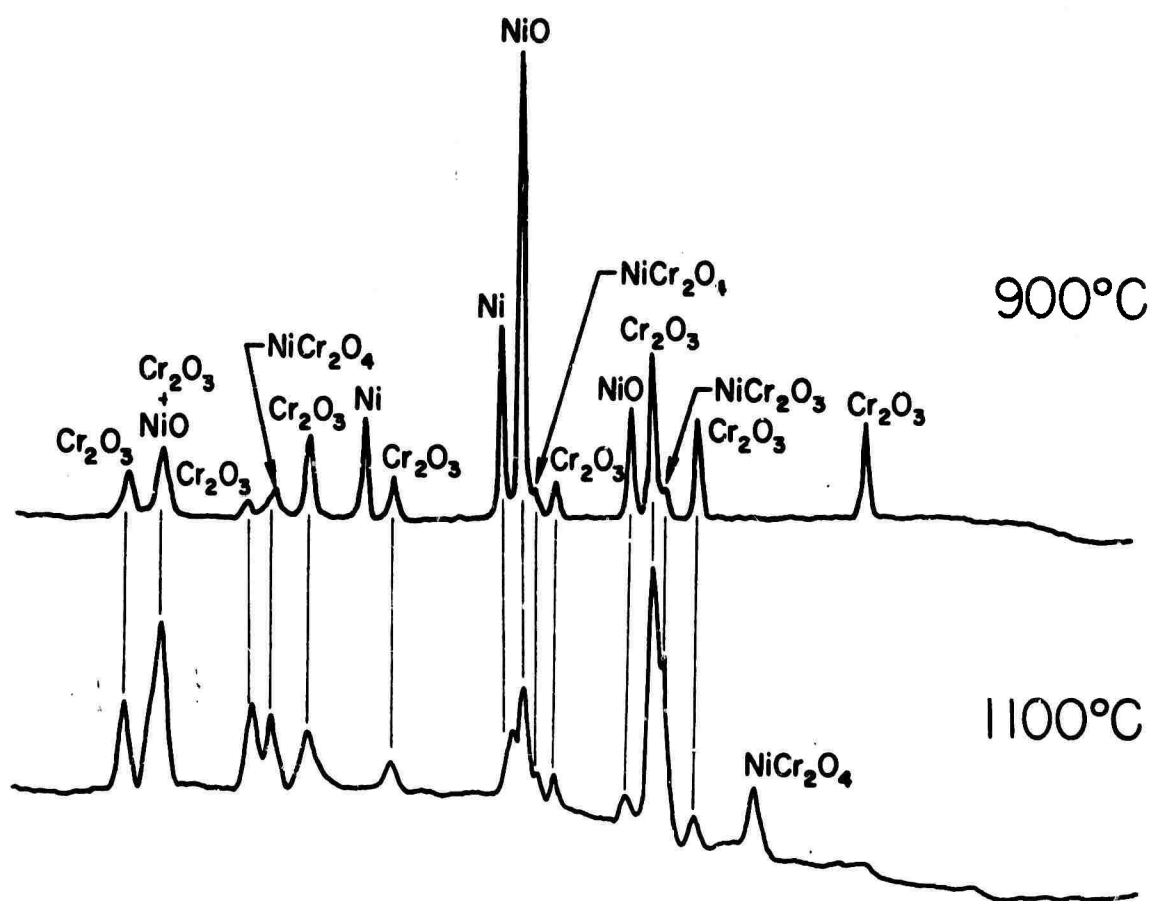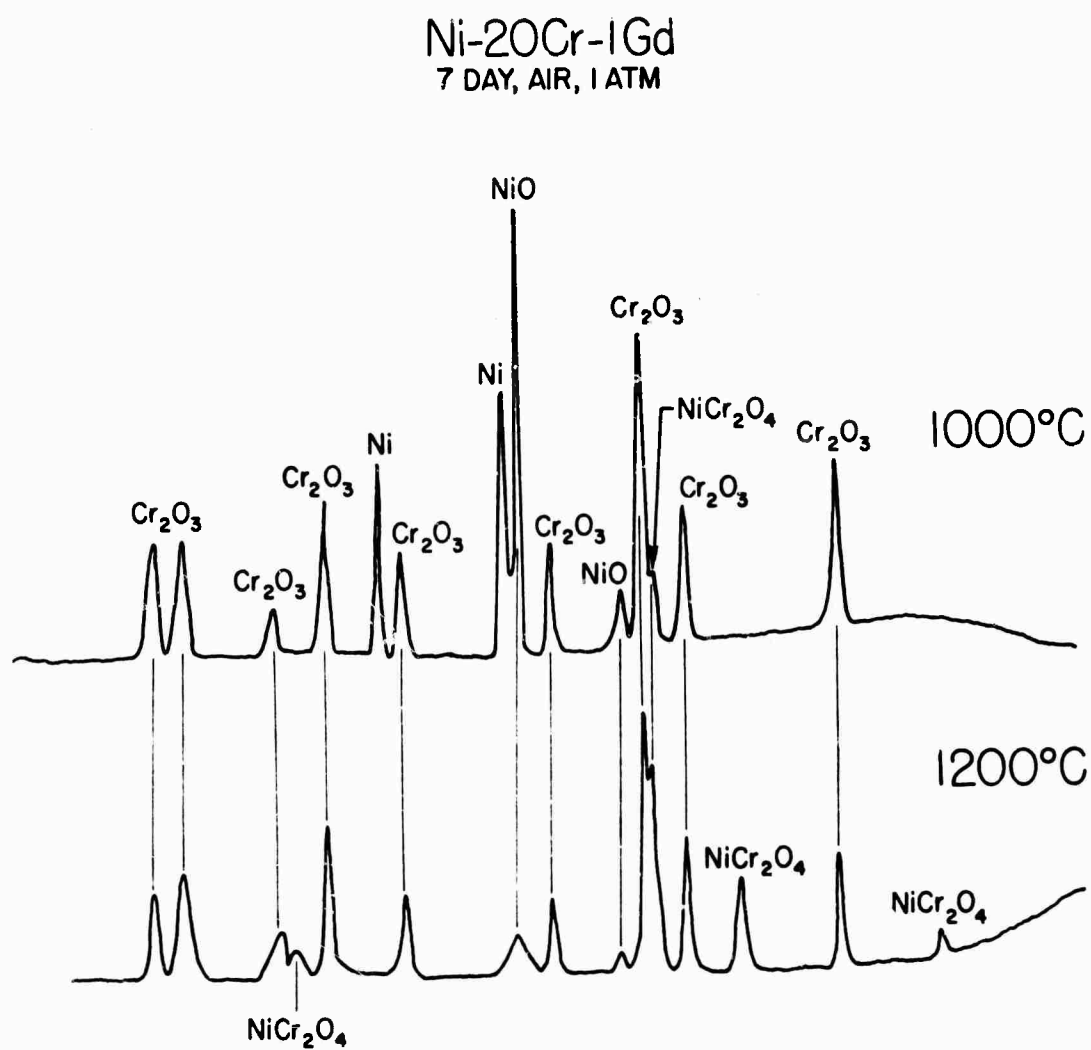
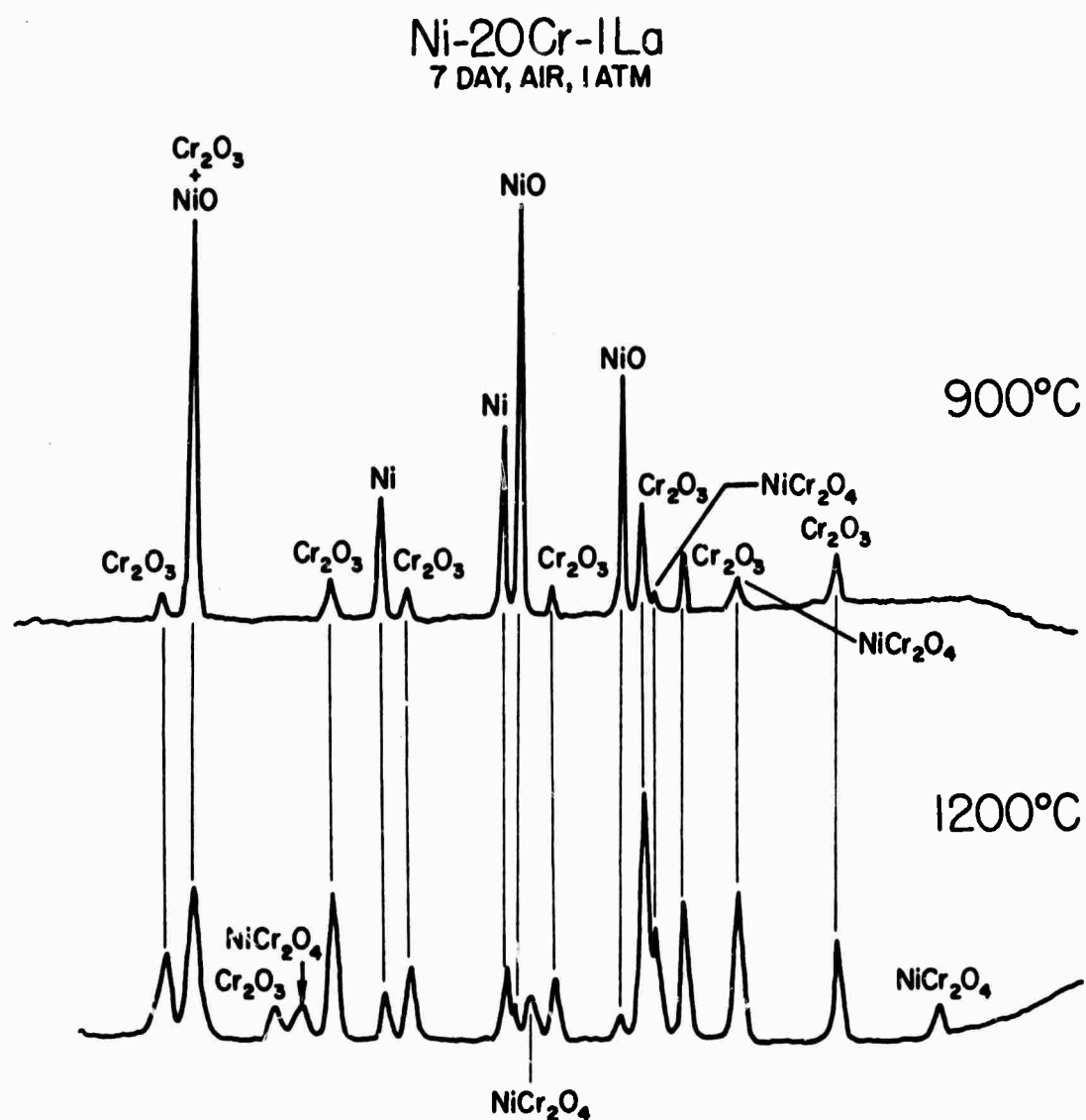**Figure 8.**   X-Ray Diffraction Patterns of Scales Formed on Ni-20Cr.

Figure 9. X-Ray Diffraction Patterns of Scales Formed on Ni-20Cr-1Gd.
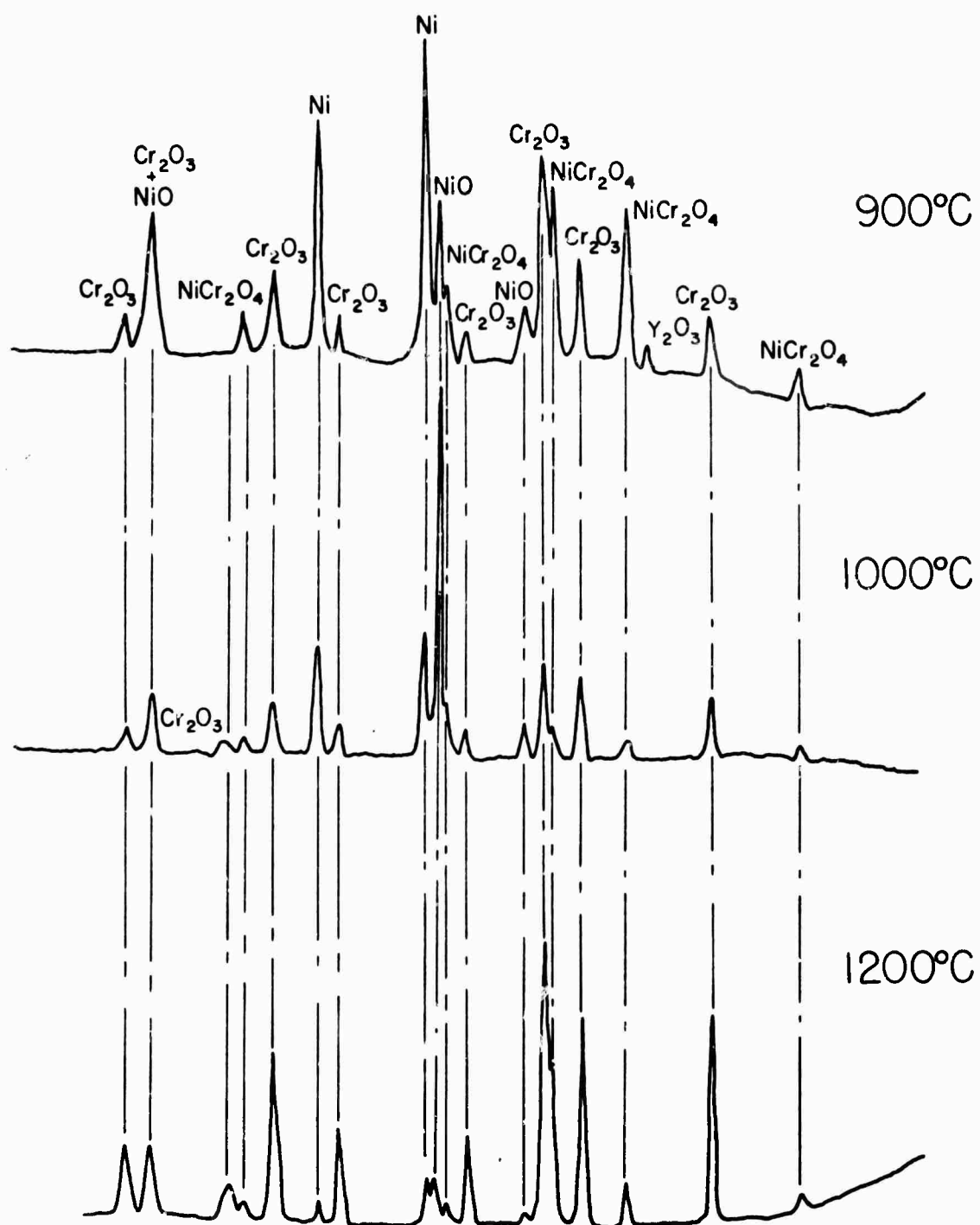
Ni-20Cr-1La
7 DAY, AIR, 1 ATM

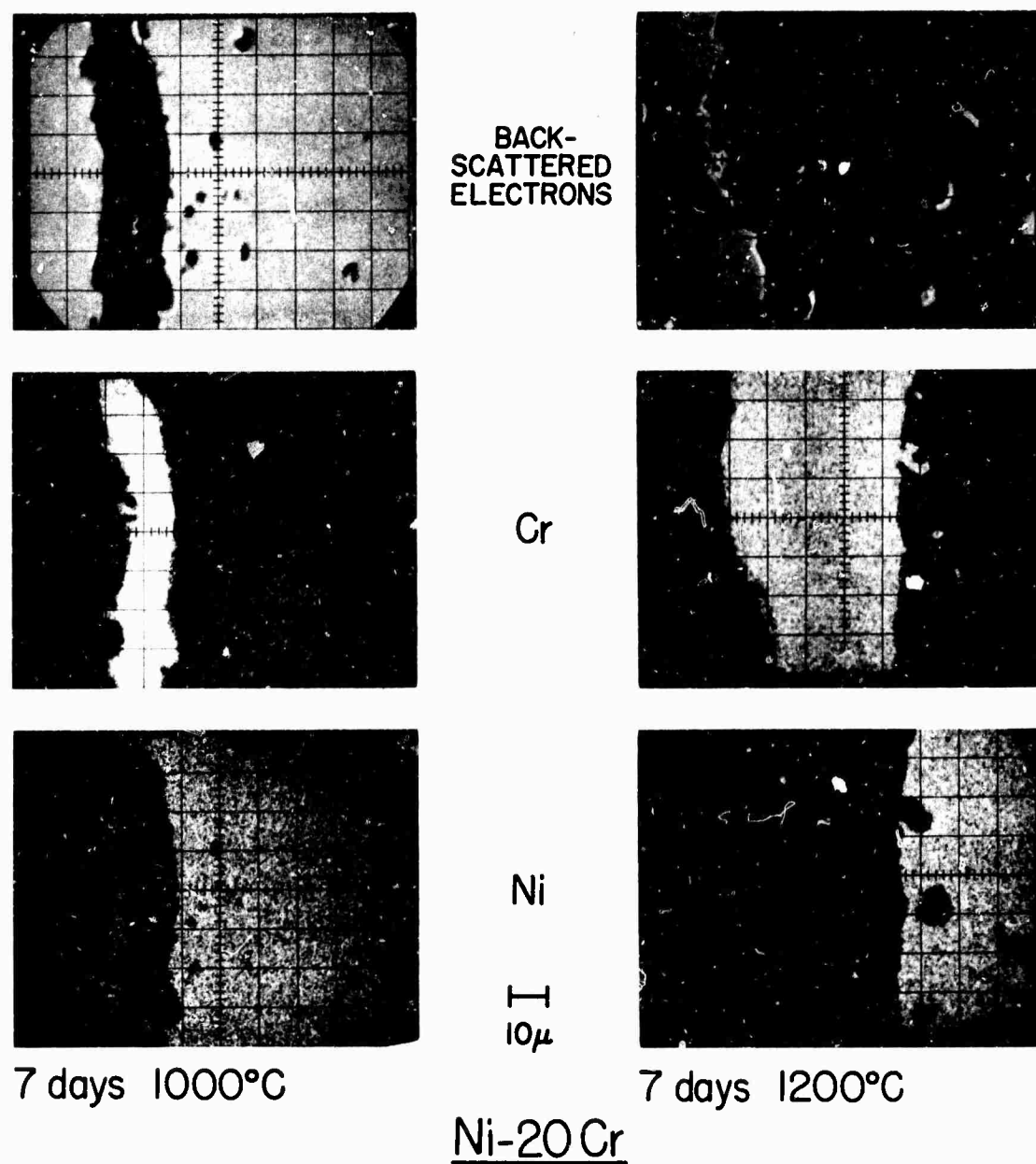Figure 10.   X-Ray Diffraction Patterns of Scales Formed on Ni-20Cr-1La.

Figure 11.   X-Ray Diffraction Patterns of Scales Formed on Ni–20Cr–1Y.

BACK-SCATTERED ELECTRONS

Cr

Ni

⊢⊣
10μ

7 days 1000°C   7 days 1200°C

Ni-20 Cr

Figure 12.   Electron Microprobe Analyses of Scales Formed on Ni-20Cr.

BACK-SCATTERED ELECTRONS

Cr

Ni

Gd

⊢──┤
10μ

7 days 1000°C

7 days 1200°C
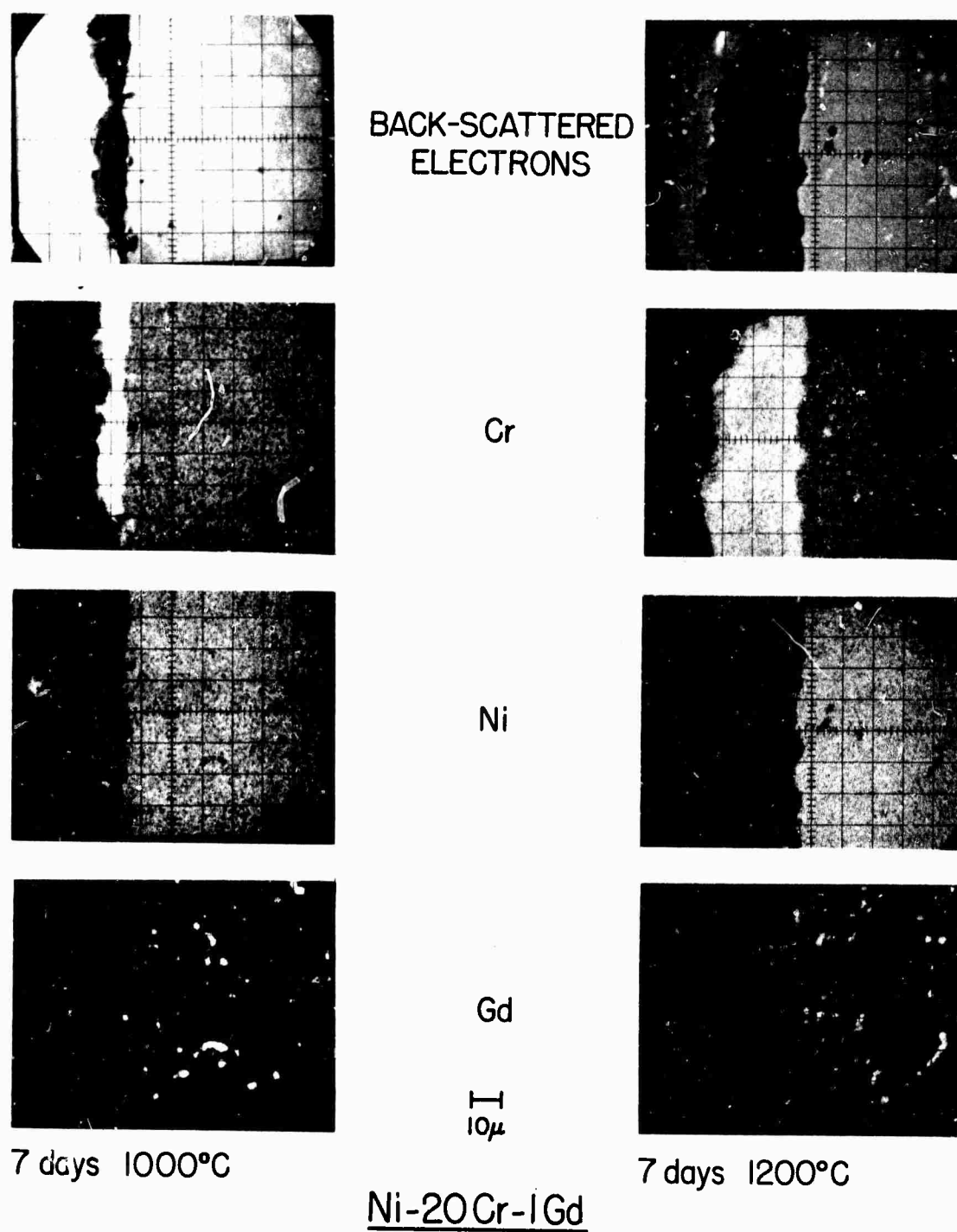
Ni-20Cr-1Gd

Figure 13.   Electron Microprobe Analyses of Scales Formed on Ni-20Cr-1Gd.

BACK-SCATTERED ELECTRONS

Cr

Ni

La

|—————|
10μ

7 days 1000°C   7 days 1200°C
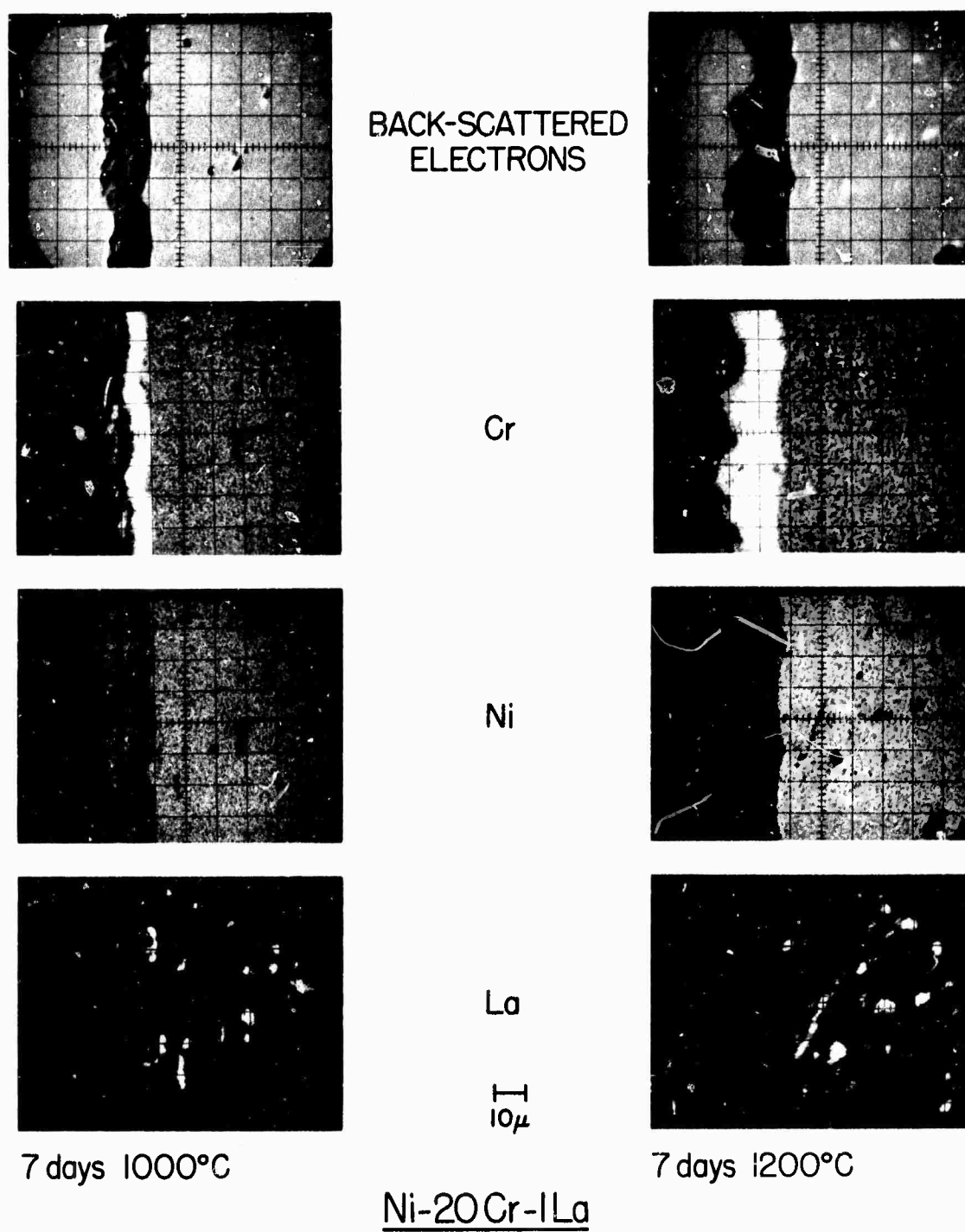
Ni-20Cr-1La

Figure 14.   Electron Microprobe Analyses of Scales Formed on Ni–20Cr–1La.

BACK-
SCATTERED
ELECTRONS

Cr

Ni

Y

$\vdash\!\dashv$
10μ

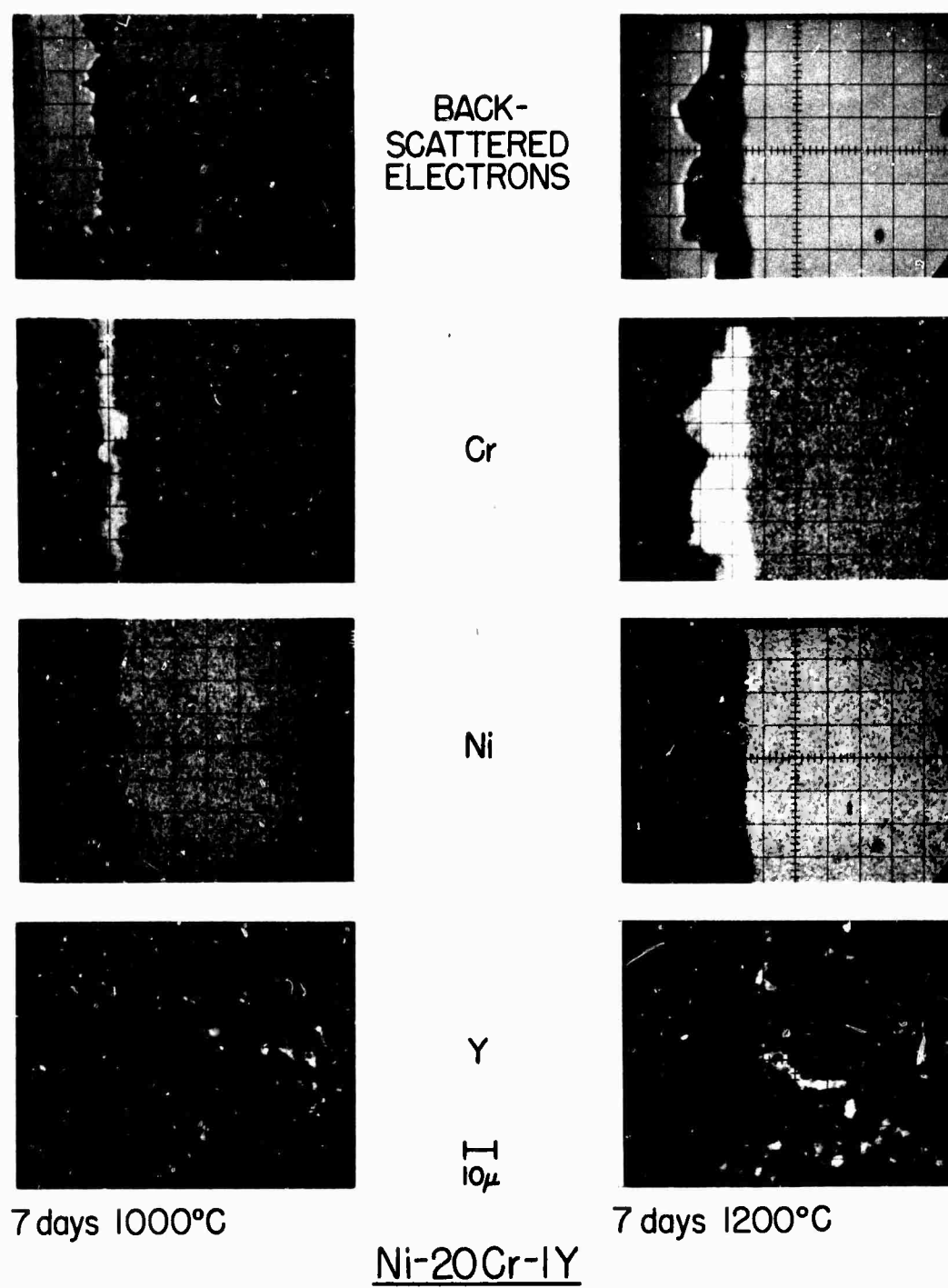7 days 1000°C   7 days 1200°C

Ni-20Cr-1Y

Figure 15.   Electron microprobe Analyses of Scales Formed on Ni-20Cr-1Y.

Discussion

The addition of certain rare earth elements to Ni-20Cr results

in a marked reduction in the oxidation rate and improved scale adherence.

The rare earths appear to stabilize Cr_2O_3 as the major film constituent

at the expense of the $NiCr_2O_4$ spinel. There does not appear to be

a measurable amount of the rare earths in the films with but one

exception previously noted.

The explanation for the above observations is not clear

presently. Previous investigators who studied rare earth effects

in Fe-Cr, Fe-Cr-Al, and Cr-base alloys have suggested various possi-

bilities, none of which are satisfactory. It is of interest, however,

to explore one mechanism which has been dismissed for erroneous

reasons, that being the "doping" effect according to the Wagner theory.

It has been stated that there should be no doping effect

because the valence of yttrium in Cr_2O_3 is 3+ the same as for Cr3+. The

Wagner theory states that only those elements having different valences

than the host cations can alter the oxide defect structure. It makes

no difference what the element is--only the valence matters. This

arises from the change in total charge by the incorporation of an

element having a different valence and the need to maintain electro-

neutrality in the crystal lattice. Electroneutrality is maintained

by the formation of or by the elimination of certain point defects,

depending on the system. For example, a p-type semiconducting oxide

such at NiO (or Cr_2O_3 if the suggested defect structure is correct)

will exhibit an increase in the cation vacancy concentration when a

higher valent solute is added such as Al or Cr, but the cation vacancy

concentration will decrease upon the addition of a lower valent

element such as lithium. These predictions are well-known and have

been experimentally verified many times.

However, the above reasoning is not complete. It is possible to change the defect concentration even though the solute valence is the same as the solvent valence. This situation can exist if the oxides have a similar structure but different enthalpies of defect formation. A notable example is NiO doped with Co. Both NiO and CoO have the NaCl-type structure and are completely isomorphous. The enthalpy for cation vacancy formation in CoO is much lower, however, than in NiO. Thus, if cobalt is added to NiO the vacancy concentration in NiO will increase because it is energetically more favorable to form vacancies. This is supported by the fact that the oxidation rate of Ni-Co alloys is greater than that of pure nickel. The parabolic rate constant is a function of the vacancy concentration which in turn effects the cation diffusion rate.

The addition of Y_2O_3 to Cr_2O_3 could actually result in a decrease in the cation vacancy concentration because the enthalpy of vacancy formation in Y_2O_3 is greater than in Cr_2O_3. This must be established experimentally, but it is highly possible.

The second erroneous reason previously mentioned concerns the level of yttrium in Cr_2O_3. If an oxide such as Cr_2O_3 is not too defective (which is actually the case), it must be extremely pure to exhibit "intrinsic" properties. Values of 0.01 to 1 ppm total impurities being representative. It is not possible to obtain oxides anywhere near this purity. Thus, Cr_2O_3 exhibits "extrinsic" properties in which case the defect concentration would be inversely proportional to the impurity content for a system in which ΔH_V solute $> \Delta H_V$ solvent. Even though the solubility of yttrium may be very low in Cr_2O_3, e.g., 100 ppm, a level of only 10 ppm could result in a ten-fold, hundred-fold, or greater reduction in the vacancy concentration, depending upon the intrinsic-extrinsic transition impurity level.

In order to check these hypotheses, it will be necessary to discern if any yttrium dissolves in the Cr_2O_3 scale, and if it does, what effect it has on chromium diffusion. The former will be established by careful point-counting with the electron micro-probe, and the latter will be evaluated by Cr^{51} tracer diffusion measurements in Y-doped Cr_2O_3.

62

Reference

1. Bunshah, R. F., and Douglass, D. L., Technical Report - UCLA-Eng-7112, March, 1971.

Personnel

The following personnel have been working on Part II of this program:

Principal Investigator - Professor D. L. Douglass

Graduate Student - Mr. J. R. Kuenzly

Figure Captions

1. Effect of testing method on the oxidation kinetics of Ni-20Cr-1Gd.

2. Comparison of x-ray diffraction patterns of oxide scales formed on samples in Figure 1.

3. Comparison of electron microprobe analyses of oxide scales formed on samples in Figure 1.

4. Oxidation kinetics of alloys tested at 1000°C.

5. Oxidation kinetics of alloys tested at 1100°C.

6. Oxidation kinetics of alloys tested at 1200°C.

7. Arrhenius plot showing temperature dependency of oxidation rates.

8. X-ray diffraction patterns of scales formed on Ni-20Cr.

9. X-ray diffraction patterns of scales formed on Ni-20Cr-1Gd.

10. X-ray diffraction patterns of scales formed on Ni-20Cr-1La.

11. X-ray diffraction patterns of scales formed on Ni-20Cr-1Y.

12. Electron microprobe analyses of scales formed on Ni-20Cr.

13. Electron microprobe analyses of scales formed on Ni-20Cr-1Gd.

14. Electron microprobe analyses of scales formed on Ni-20Cr-1La.

15. Electron microprobe analyses of scales fromed on Ni-20Cr-1Y.